Earth-Science Reviews 115 (2012) 304–318

Contents lists available at SciVerse ScienceDirect

Earth-Science Reviews

journal homepage: www.elsevier.com/locate/earscirev

What can physical source models tell us about the recurrence time of earthquakes?

Andrea Bizzarri *

Istituto Nazionale di Geofisica e Vulcanologia, Sezione di Bologna, Italy
Via Donato Creti, 12, 40128 Bologna, Italy

ARTICLE INFO

Article history:
Received 29 June 2012
Accepted 8 October 2012
Available online 24 October 2012

Keywords:
Earthquake source dynamics
Earthquake recurrence
Rheology of faults
Computational seismology
Characteristic earthquake

ABSTRACT

Earthquake prediction, no matter what the timescale, has been and continues to be a contentious subject and it is indubitably a prominent challenge for modern seismology and earthquake physics. Indeed, few natural events can have the catastrophic consequences of earthquakes (earthquakes today account for about 60% of natural fatalities). A physical description of an earthquake represents an amenable approach to the prediction, but it suffers of some limitations, basically due to the notorious ignorance about the initial state of a given fault and about the physical law controlling its traction evolution. Independent on those intrinsic, epistemic limitations, the concept of the earthquake recurrence, based upon the idea of the cyclic (or characteristic) earthquake, has been often invoked to describe (and thus to predict) subsequent instability events on a seismogenic structure. In this paper, by using the simplest analog fault model, the one-degree-of-freedom mass–spring system, we quantitatively show that the concepts of the recurrence time and the earthquake cycle have limitations (even making them meaningless). We will discuss in a compendious synopsis all the possible physical mechanisms which can dramatically affect the recurrence time. Our conclusions emphasize again that the competing mechanisms potentially occurring during faulting, even in the simplest and idealized condition of an isolated fault, can significantly complicate the regular cyclicity of earthquakes predicted by the analog fault system. These conclusions can contribute to the debate about the role of the physical modeling of earthquakes in the contest of seismic hazard assessment.

Contents

* Istituto Nazionale di Geofisica e Vulcanologia, Sezione di Bologna, Italy. Tel.: +39 051 4151432; fax: +39 051 4151499.
E-mail address: bizzarri@bo.ingv.it.

0012-8252/$ – see front matter
http://dx.doi.org/10.1016/j.earscirev.2012.10.004

1. Introduction

The time of occurrence of earthquakes has clear implications in the context of seismic hazard assessment (SHA), and disaster mitigation and it has a major relevance in the framework of the physics of faulting. The concept of the self-organized criticality (SOC) assumes that the Earth's crust is always in a critical state in terms of stress conditions (Bak et al., 1987; Turcotte, 1997; Turcotte et al., 2009). The SOC idea can give an explanation of the scale-invariant power-law behaviors frequently recognized in real earthquakes described by the Gutemberg–Richter (Gutenberg and Richter, 1944) recurrence law for the magnitude distribution of the earthquake events and the Omori law (Jeffreys, 1938) for the time evolution of the frequency of the aftershocks (see also Scholz, 2002; Rundle et al., 2003; Turcotte et al., 2009). Both of these empirical laws are essentially of statistical nature, in that they become evident only after examining a sufficiently large number of events. A common example of this kind of stochastic models is the decision-making process, as well as the statistical mechanics (see for instance Vere-Jones, 2010). In seismology, the probabilistic methods often presents a lack of knowledge about the physical processes behind an earthquake and this is the reason of criticism expressed by some authors (e.g., Wang, 2008, among others).

On the other hand, it should also be mentioned that, sometimes, real earthquakes exhibit apparently opposite features, in that they are commonly referred to as "characteristic earthquakes" (CEs). This concept, basically formalized by Reid (1910) and build on a letter to the Salt Lake City Tribune in 1883 by G. K. Gilbert, assumes that a dynamic event occurs in the Earth crust when the tectonic shear stress reaches some critical level, at regular time intervals, determined by the state of the fault and by the tectonic load (see also Schwartz and Coppersmith, 1984). Classical models of earthquake recurrence (e.g., Shimazaki and Nakata, 1980) postulate that the time of occurrence of the next earthquake event can be somehow predicted a priori, given the critical level of stress (strictly periodic or time-predictable models) or the stress drop that occurred during the previous event (slip-predictable models). The CE model theorizes that the Gutemberg–Richter relationship does not hold for large interplate earthquakes that do not represent the distribution of seismicity on an individual fault (Ishibe and Shimazaki, 2012, and references cited therein).

The concept of earthquake recurrence is intimately related to the concepts of seismic cycle, which becomes popular because several earthquakes have been observed to occur in the same segment of the fault with nearly constant inter-event times; off Kamaishi, where the Pacific plate subducts beneath northern Honsu, Japan, magnitude 4.8 ± 0.1 earthquakes occurred repeatedly at intervals of 5.5 ± 0.7 years since 1957 (Okada et al., 2003). Sykes and Menke (2006) found that great earthquakes of magnitude 8 occurred along the Nankai trough, where the Philippine Sea plate subducts beneath southwestern Japan, roughly every 100 years. Moreover, at the Parkfield segment of the San Andreas fault, California, interplate earthquakes of about class 6.0 have occurred at recurrence intervals of 23 ± 9 years since 1857 (Bakun and McEvilly, 1979; Sykes and Menke, 2006). Moreover, the concept of recurrence time is widely used in probabilistic hazard analysis and has also practical implications, in that it forms the basis of building codes in many countries, including Italy; indeed, the technical rules of building construction in Italy (Norme tecniche di costruzione, 2008) are presently based upon the concept of recurrence time (see Table 1 therein), because they rely on the probabilistic seismic hazard assessment (PSHA). Moreover, the concept of recurrence time is also employed in the framework of earthquake prediction.

There is no reason to overemphasize that in the framework of the seismology the physical modeling is inherently amenable. However, there are two main limitations in this kind of approach to describe the earthquake faulting: (1) the ubiquitous ignorance of the initial state of the faults, expressed both in terms of stress state and geometrical features, and (2) the ignorance of the governing laws describing the dissipative chemico-physical mechanisms potentially occurring (and interacting one with another) during an earthquake failure. Both of these limitations pose an outstanding challenge to both seismologists and physicists; a thorough discussion can be found in Bizzarri (2009, 2011a). An illustrative, albeit oversimplified, example can be found in the behavior of a bullet; if we exactly know the initial velocity, the angle with respect to the horizontal and the initial direction, then the knowledge of the second law of dynamics makes it possible for us to exactly predict where and when the bullet will hit the ground. In the mechanics of faulting we still ignore the exact law which controls the traction evolution before, during and after a seismic event. Since the early knowledge of '70s and '80s (far of being exhaustive, see for instance Ida, 1972; Dieterich, 1978; Ruina, 1983) much progress has been made both in laboratory investigations (e.g., Sone and Shimamoto, 2009 among many others) and in numerical experiments (Bizzarri, 2011a; Lapusta and Barbot, 2012). An important point has to be stated here; in quantum mechanics the Heisenberg's uncertainty principle theoretically established the impossibility to exactly predict the position and the momentum of a particle, simultaneously (Heisenberg, 1927). On the contrary, there is no *theoretical* reason to state that the prediction of an earthquake occurrence is a priori impossible from a theoretical point of view. Of course, the serious (practical) limitations discussed above make this ambitious goal tremendously far of being nowadays accomplished and the result is that, as at today, there is no reliable method available to predict earthquakes in a strict direct (or forward), deterministic sense. With the term deterministic we refer to physical models in which all the components of the mechanical system can be described through the formulation of mathematical laws and its behavior can be therefore predicted exactly. We distinguish this approach from the stochastic (or statistical) models, which accept that several properties of a given process are out of range, and that they are replaced by random processes, whose behavior cannot be predicted exactly (as in the previous case), but can be described only in probability terms (Vere-Jones, 2010).

In this paper we critically review the concept of recurrence time and analyze the applicability of this concept on the knowledge that can be gained from the study of basic physical fault models. In particular, we will consider a physical approach, in which the fault governing law and the initial condition are assumed to be known (see Section 2). By considering different mechanisms occurring during faulting (Sections 3–8) we will explore if this time can be properly defined and we quantitatively show how much it can be constrained. In Sections 9 and 10 we summarize the results and we discuss the potential implications.

2. The physical modeling of repeated earthquakes

2.1. The spring–slider dashpot model

In this paper we consider the widely-employed 1-D fault model, known as spring–slider (or mass–spring) system, in which the fault is modeled as a material point of mass m (per unit area), which slides over a plane against a frictional resistance τ and it is subjected to a normal load σ_n^{eff} (see for instance Gu et al., 1984; Tse and Rice, 1986, among many others). The system is loaded at the end of the spring by a remote velocity, v_{load}, which physically represents the speed of a tectonic plate loading the seismogenic region under study. A sketch of the system is reported in Fig. 1.

The equation of motion of the spring–spider system is a first order PDE describing a damped harmonic oscillator:

$$\dot{\mathbf{U}} = \mathbf{F}(\mathbf{U}, t) \tag{1}$$

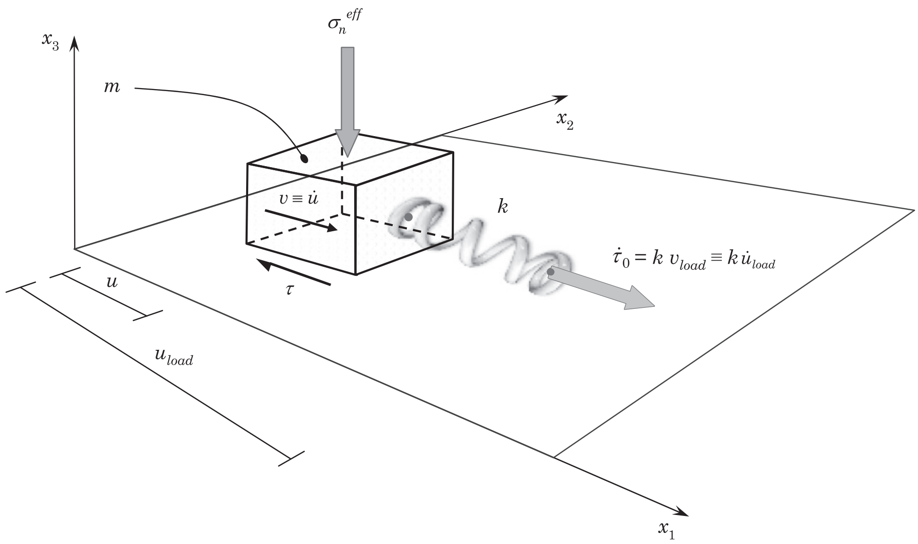

Fig. 1. Sketch representing the mass–spring fault model adopted in this paper. A mass m (per unit fault surface area) is loaded by a remote tectonic load $\dot{\tau}_0 = k\, v_{load} \equiv k\, \dot{u}_{load}$ exerted through a spring of elastic constant k (v_{load} is the velocity of the tectonic plate). The mass slides on the plane (simulating the fault) against a frictional resistance τ. Modified from Bizzarri (2010).

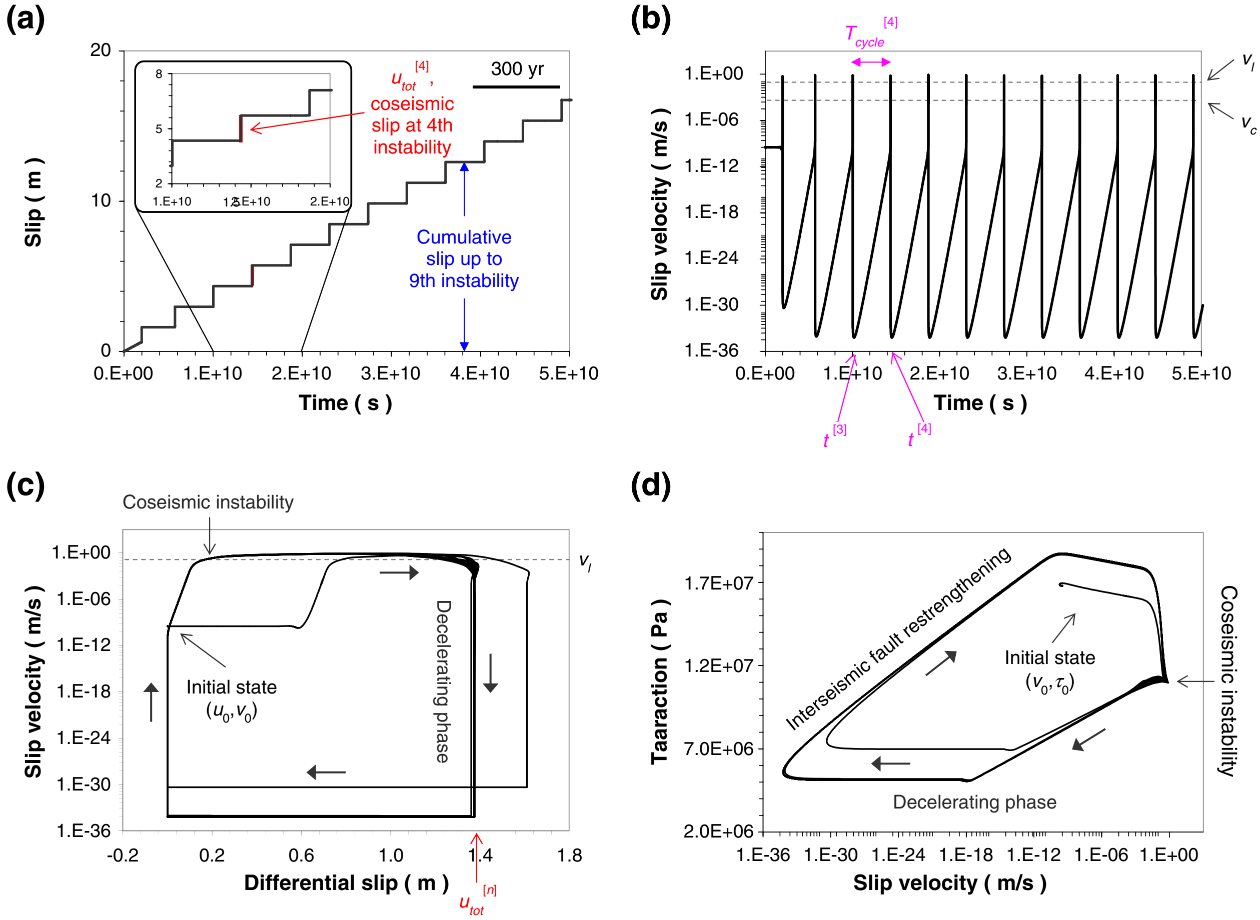

Fig. 2. Results pertaining to a spring–slider simulation with the canonical Dieterich–Ruina law (Eq. (33) in Bizzarri, 2011a) and the parameters of Table 1. (a) Time evolution of the slip, with inset reporting a zoom of the region marked in gray in panel (a). (b) Time evolution of the slip velocity, in semi-logarithmic scale. (c) Phase diagram in the space (u,v). In the abscissa we report the slip developed during each instability event, i.e. the quantity $u(t) - u_{tot}^{[n-1]}$, for $t \geq t^{[n-1]}$. (d) Phase diagram in the space (v,τ). In panels (c) and (d) black arrows indicate the direction of the orbit. (For interpretation of the references to color in this figure, the reader is referred to the web version of this article.)

where

$$\mathbf{U} \equiv \begin{bmatrix} u \\ v \end{bmatrix} \quad \text{and} \quad \mathbf{F} \equiv \begin{bmatrix} v \\ \frac{1}{m} f(u, v, t) \end{bmatrix} \tag{2}$$

with

$$f(u, v, t) \equiv k v_{load} t - k u(t) - \tau. \tag{3}$$

In Eq. (1), **U** formally defines the state of the system at a generic time *t*, in the canonical phase space (*u*,*v*), which is, for fault models, the counterpart of the canonical phase space (*p*,*q*) in classical Hamilonian systems (*p* is the position of a material point and *q* is its momentum; e.g., Findlay, 1911). The overdot in Eq. (1) indicates the time derivative. In Eqs. (2) and (3) *u* is the displacement of the block and *v* is its time derivative (i.e., the sliding velocity). Namely, the quantity *u* defines how much the fault has slipped at a generic time *t* (see also next Fig. 2a). Although there is no explicit discontinuity interface in the present model, during the coseismic phase of the rupture (characterized by the "slip" event) *u* can be regarded as the fault slip, properly defined in continuum models of faulting as the discontinuity of the displacement vector (see Eq. (3) in Bizzarri, 2011a). The velocity *v* spans over many orders of magnitude, characterizing the slow interseismic phase (or the "stick" phase of the dynamical system, in which $v \sim v_{load}$) and the coseismic stage (in which *v* approaches the so-called seismic range, where $v \sim$several m/s). The fault stiffness *k* – which mimics the interactions with the elastic medium surrounding the fault – can be associated with the static stress drop and the total slip developed during the failure event (Walsh, 1971). The constants *m* and *k* define the period of the freely slipping harmonic oscillator, $T = 2\pi\sqrt{\frac{m}{k}}$. Finally, the product kv_{load} expresses the loading rate of tectonic origin ($\dot{\tau}_0$), which is a constant in the present model.

The traction τ appearing in Eq. (3) formally defines the fault governing law, which is an analytical relation expressing the dependence of the shear stress components on some physical observables, such as *u*, *v*, some state variables, etc. In full of generality, we can express τ as in Eq. (10) of Bizzarri (2011a); in the remainder of the paper we will refer to the rate- and state-dependent rheology (Ruina, 1983).

Eqs. (1)–(3) are a proxy of the true behavior of an extended fault embedded in a continuous medium and they are intended to be valid in the case of a fault with homogeneous properties. More complicated – and realistic – models can be formulated to study the whole life of a fault; for instance, the inherently discrete Burridge–Knopoff model (Burridge and Knopoff, 1967), in which multiple blocks of mass are connected by springs having potentially different elastic constants to mimic the possible spatial heterogeneities in the elastic medium (Huang et al., 1992), can be regarded as a natural extension of the single body spring–slider system considered here (see also Kawamura et al., 2012 for a discussion). The Burridge–Knopoff model becomes very popular in the physics community after Carlson and Langer (1989a, 1989b), because of its capability to reproduce the Gutemberg–Richter law (e.g., Saito and Matsukawa, 2007). On the other hand, we mention that models of finite-extend fault have been also adopted to simulate the quasi-static and the subsequent quasi-dynamics stages of an earthquake rupture (e.g., Lapusta and Liu, 2009). In the present study we deliberately adopt the simplest model to simulate the evolution of the fault properties to better focus on the concept of earthquake recurrence, without considering the possible complications arising from spatial heterogeneities and geometrical complexity of fault structures handled in extended fault models.

2.2. Dynamic instabilities and seismic cycle

To define the inter-event time we must define the time occurrence of an instability. To this goal we introduce a threshold value of the sliding velocity (v_l); when *v* exceeds v_l we define the time occurrence of an earthquake instability:

$$t^{[n]} \left| v\left(t^{[n]}\right) \geq v_l \right. \tag{4}$$

where the integer *n* counts the number of instabilities. This threshold criterion has been widely adopted in the previous literature (Day et al., 2005; Rubin and Ampuero, 2005; Bizzarri and Belardinelli, 2008; Bizzarri and Spudich, 2008), because it has the relevant advantage of being independent on the value attained by the fault traction, which is a priori knowable in the framework of the linear slip-weakening friction law (Ida, 1972), but is a priori unpredictable in the case of the rate- and state-dependent friction laws (Bizzarri et al., 2001; Bizzarri and Cocco, 2003).

The time separating two subsequent instability events naturally defines the seismic inter-event time (T_{cycle}), which of course has a different meaning than the period *T* defined in Section 2.1. We can write (for $n \geq 2$):

$$T_{cycle}^{[n]} \underset{df}{=} t^{[n]} - t^{[n-1]}. \tag{5}$$

2.3. Numerical approach

Although the equation of motion (1) can be solved analytically in a closed-form for some special cases (see Bizzarri, 2012a), we solve it numerically by using the fourth-order accurate Runge–Kutta algorithm with auto-adaptive time stepping (Press et al., 1992). Our numerical code, which implements the algorithms RKQC and RK4 of Press et al. (1992), gives the same results as the ODE45 routine in Matlab® (see Matlab® documentation), used by other authors (e.g., Kato, 2001; de Lorenzo and Loddo, 2010).

We consider two different regimes of the dynamical system, one being characterized by a quasi-static behavior and one which is fully dynamic. They are discriminated by a critical value $v_c \ll v_l$; for $v \geq v_c$ we solve the complete equation of motion (Eq. (1)), while for $v < v_c$ we neglect the inertial affects. In this case we assume that the sliding acceleration is negligible because the fault is evolving slowly; this stage basically represents the interseismic phase of the fault, described by the following equations

$$\dot{\tilde{\mathbf{U}}} = \mathbf{F}(\mathbf{U}, t) \tag{6}$$

where:

$$\tilde{\mathbf{U}} \equiv \begin{bmatrix} u \\ 0 \end{bmatrix} \tag{7}$$

and **F** is the same as in Eq. (2). By considering the definition of *f* (see Eq. (3)), Eq. (6) can be simply written as it follows:

$$k v_{load} t - k u(t) - \tau = 0. \tag{8}$$

2.4. A typical example of a characteristic earthquake

An example of the evolution of the system is reported in Fig. 1; the parameters are tabulated in Table 1. In this case we adopt the canonical (or classical) formulation of the Dieterich–Ruina (DR henceforth) law (see Eq. (33) in Bizzarri, 2011a and references cited therein). In this example we can clearly envisage the cyclic behavior of the

Table 1
Reference constitutive parameters adopted in this study. The subscript 0 denotes the initial state of the system, at $t=0$.

Parameter	Value
Model parameters	
Tectonic loading rate, $\dot{\tau}_0 = kv_{load}$	3.17×10^{-3} Pa/s (=1 bar/year)
Machine stiffness, k	10 MPa/m [a]
Period of the analog freely slipping system, $T=2\pi\sqrt{m/k}$	5 s
Critical value of the sliding velocity above which the dynamic regime is considered, v_c	0.1 mm/s
Threshold value of the sliding velocity defining the occurrence of an instability, v_l	0.1 m/s [b]
Fault constitutive parameters	
Initial effective normal stress, $\sigma_n^{eff}{}_0$	30 MPa
Logarithmic direct effect parameter, a	0.007
Evolution effect parameter, b	0.016
Characteristic scale length, L	1×10^{-2} m
Reference value of the friction coefficient, μ_*	0.56
Reference value of the sliding velocity, v_*	3.17×10^{-10} m/s
Initial slip velocity, v_0	3.17×10^{-10} m/s
Initial value of the state variable, Ψ_0	31.5×10^6 s (=$\Psi^{ss}(v_0)=L/v_0$) [c]
Initial shear stress, τ_0	16.8 MPa (=$\mu_*\sigma_n^{eff}{}_0$)

[a] With the adopted constitutive parameters this corresponds to an unstable regime, in that $k<k_{cr}\equiv(b-a)\sigma_n^{eff}/L=27$ MPa/m (Gu et al., 1984).
[b] In agreement with Bizzarri and Belardinelli (2008) and references cited therein.
[c] The system starts at $t=0$ from its steady state (at a generic time t_* the steady state is defined by the condition $\frac{d}{dt}\Psi|_{t=t_*}=0$).

system; the slip developed during a single instability, $u_{tot}^{[n]}$, is always the same (Fig. 2a), as well as $T_{cycle}^{[n]}$ (Fig. 2b; in this case 138 years). This is due to the fact that, after the completion of the evolutionary phase, related to the initial conditions, the system enters in its limiting cycle (Fig. 2c and d). In particular, we have that the values attained by the traction during subsequent instability events are the same, in that the peak and the minimum stresses are the same. This guarantees the same stress release during each instability, which reflects in the same magnitude of the earthquakes occurring on this fault. Also the minimum values of the slip velocity are constant through time (Fig. 2b) and this causes the restrengthening phase to be always the same. In other words, the fault takes always the same time to recover its stress and reach the failure point at the next instability event. We can clearly see in the phase portraits (Fig. 2c and d) that the same trajectory (or orbit) in the phase space is covered forever, after the transient, initial stage. Mathematically, if we denote with $\mathbf{S}(t)$ a generic state of the system (which can be either $\begin{bmatrix} u(t)-u_{tot}^{[n-1]} \\ v(t) \end{bmatrix}$ or $\begin{bmatrix} v(t) \\ \tau(t) \end{bmatrix}$ referring to Fig. 2c and d, respectively), we have that $\mathbf{S}_{cycle}$ is the limiting cycle, because it holds:

$$\lim_{t\to+\infty} ||\mathbf{S}(t)-\mathbf{S}_{cycle}|| = 0. \tag{9}$$

It is apparent that this numerical experiment represents the prototype of a cyclic, or characteristic, earthquake. In the following Sections 3–8 we will discuss how much this idealistic configuration is realistic and whether it is a stable feature emerging from dynamic modeling of earthquakes.

3. Fault interactions and stress triggering

A fault is not an isolated physical system, but it is generally a part of a more complex environment, where multiple faults interact one with the others. Indeed, when a fault fails the emitted seismic waves not only strike the ground, but also perturb the Earth (e.g., Harris, 1998; Stein, 1999). These stress perturbations can be responsible for aftershocks and they can also trigger earthquakes in the neighboring areas. The stress re-distribution can broke "asperities" (Kanamori, 1981) prone to fail or load damaged zones characterized by different levels of instability (Boatwright and Cocco, 1996). Depending on their features, different stress perturbations can trigger "new" earthquake events in a very elaborated way (Belardinelli et al., 2003); at remote distances transient (i.e., dynamic) stress changes are dominant (Rybicki et al., 1985; Cotton and Coutant, 1997; Gomberg et al., 1997), but in the near-field transient and permanent (i.e., static) stress changes cannot be separated and they act together in triggering impending earthquakes (Harris, 1998; Gomberg et al., 2000).

It is evident that even if we postulate the theoretical existence of the cycle time of an earthquake, its cyclicity can be dramatically altered by other events previously occurred. This argument alone is able to explicitly state the serious theoretical limitation in the concept of the characteristic earthquake recurrence. In the remainder of the paper (Sections 4–8) we will consider only a single fault and we will concentrate on the various things which can affect T_{cycle} or even make it meaningless.

4. The role of the assumed governing model

In the present section we will show that the recurrence time inherently depends on the choice of the constitutive law. Actually, the choice of the most appropriate model to describe the physics of earthquakes is still a matter of lively debate. The discussion of the limitations and the major advantages of the various friction laws inferred from laboratory experiments or introduced theoretically are definitively beyond the scope of the present paper; readers can refer to the thorough review in Bizzarri (2011a).

To show how much T_{cycle} can vary depending on the adopted governing equation we have considered three different constitutive models, namely, the DR, the Ruina–Dieterich (RD hereinafter) and the Chester–Higgs (CH hereinafter) models (see Eqs. (33), (35) and (48) of Bizzarri, 2011a, respectively). The DR and RD models basically differ for the formulation of the evolutionary law for the state variable; in the former the state variable Ψ describes the time evolution of the micro-asperity contacts, while in the latter it has to be regarded simply as a dummy variable, which accounts for the memory of the previous slip events (Ruina, 1983). On the other hand, the CH model descends from the RD one, but it incorporates an explicit dependence of the frictional resistance on the temperature T developed by frictional heat. In this case T appears as a third, independent variable (in addition to v and Ψ) in the analytical formulation of τ. (In Section 8 we will discuss an alternative interpretation of the temperature-dependence of τ, in which T enters in the constitutive parameters, which is constant in the present modeling.) All of the above-mentioned governing models, basically inferred from experiments at laboratory-scale, have been assumed to be valid also at real fault-scale; indeed, there seems not to be an obvious distinction between the source physics underlying small and large events (Zechar and Nadeau, 2012).

Figs. 3 and 4 summarize the results of numerical simulations. In these figures we have also considered, for each evolution law, a modification at high speeds, in which the explicit dependence on v of the frictional resistance is assumed to be valid only at low speeds (Weeks, 1993; Boatwright and Cocco, 1996; Mitsui and Cocco, 2010; Bizzarri, 2012c), Namely, it is assumed that the term $\ln(v/v_*)$ is replaced by $\ln(v_c/v_*)$ for $v\geq v_c$ (i.e., in the dynamic regime; see Section 2.3). From the evolution of the sliding velocity (Fig. 3a) we can note the differences between the velocity peaks for each constitutive law, as well as the different time occurrence of seismic events obtained by assuming the same constitutive law on the fault, but considering frozen or not frozen conditions. In particular, referring to the velocity peaks, we can see that higher velocities are reached in the case of the DR law. Furthermore, the slip velocities obtained for the frozen

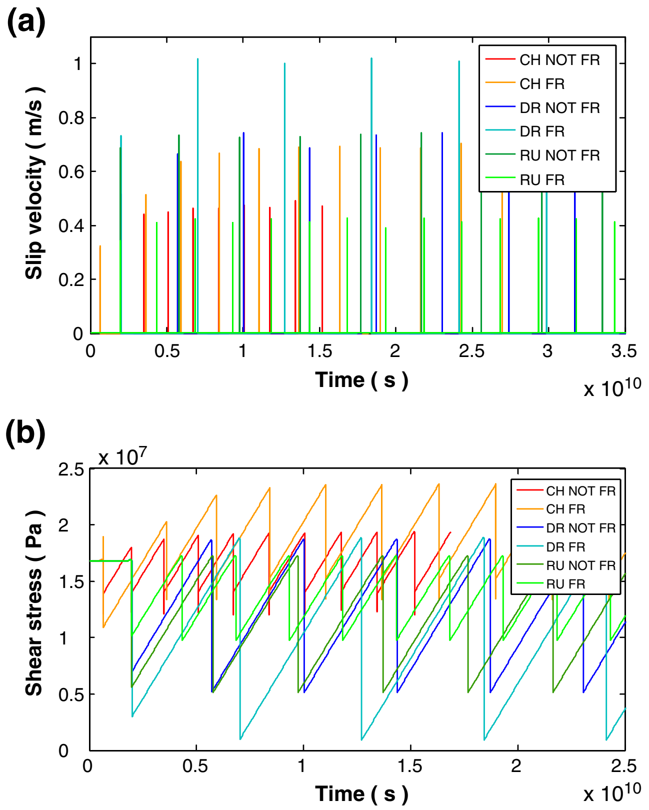

Fig. 3. Time evolution of the sliding velocity (panel (a)) and traction (panel (b)) resulting from different governing models. Open symbols refer to the frozen simulation while those closed refer to the not frozen simulation (see Section 4 for details). The parameters are those of Table 1; in the case of CH law the additional parameters are: $T_0=100$ °C, $c=2.6\times10^6$ J/(m^3 °C) and $\kappa=1\times10^{-6}$ m^2/s. The temperature due to frictional heat is computed following Eq. (3) of Bizzarri (2010) in the limit of vanishing slipping zone thickness w (in this case we maximize the effects of T in the expression of τ).

case are greater than those obtained for the not frozen one, for both DR and CH constitutive laws, while an opposite trend occurs for the RD law.

We plot in Fig. 2b the time evolution of the resulting traction predicted by the different constitutive equations. It can be clearly observed that higher shear stress peaks are obtained with the CH frozen simulation (light red line), while lower shear stress peaks are reached in the RD simulations (light and dark green lines). Moreover, the shear stress peaks reached in both DR an RD simulations are comparable, while the CH frozen peaks are significantly greater than those referred to the CH not frozen simulation. Furthermore, by considering both the DR simulations (frozen and not frozen; light and dark blue lines), the shear stress minima are significantly lower in the frozen constrain. The opposite occurs in the RD simulations, that is the minima turn out to be lower in the not frozen case. On the other hand, the traction minima seem to be comparable in both the CH simulations. Interestingly, the stress drop pertaining to each constitutive law is proportional to the slip velocity peaks (showed in Fig. 3a); the highest stress drops are associated to the highest slip velocities, realized in the DR simulations.

To the present matter the most apparent result is reported in Fig. 4, which shows the recurrence times of the seismic instabilities for all the considered constitutive laws, either in frozen and not frozen case. Here it can be observed that, on average, for both the frozen and not frozen simulations the CH law shows a lower seismic cycle pattern, the DR shows the highest values of seismic cycle while the RU seismic cycle is about in the middle. Moreover, while for both CH and DR laws the seismic cycle is smaller in the not frozen case, for the RD law the lower seismic cycle is related in the frozen

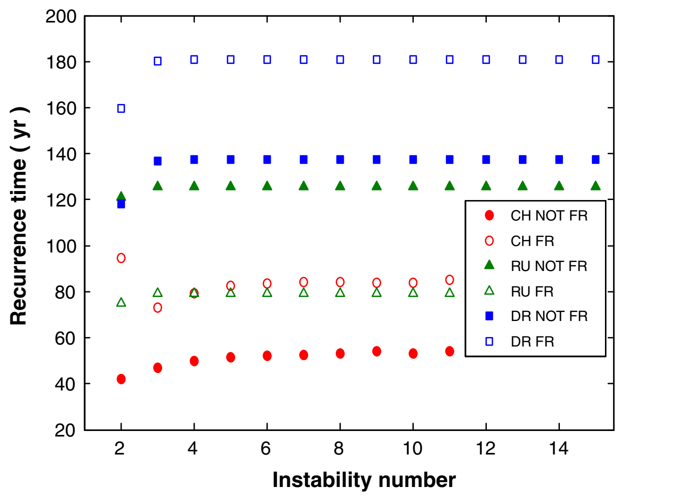

Constitutive law	T_{cycle} (yr)	$(T_{cycle}^{(FR)}-T_{cycle}^{(NOT\ FR)})/T_{cycle}^{(FR)}$ (%)
Dieterich–Ruina frozen	181	0.24
Dieterich–Ruina	138	
Ruina–Dieterich frozen	79	− 0.58
Ruina–Dieterich	126	
Chester–Higgs frozen	84	0.36
Chester–Higgs	54	

Fig. 4. Recurrence times (T_{cycle}) pertaining to the cases sown in Fig. 3. T_{cycle} is computed in all cases starting from the 5th instability event, in order to avoid possible effects of the transient stage of the system, basically controlled by the initial conditions. The table summarizes the values of T_{cycle}.

simulation. Therefore the RU seismic cycle has an opposite trend, compared to the other two constitutive laws, as it can be from Fig. 4.

The most prominent conclusion of the present exercise is that, although constant over the whole live of the fault, the recurrence time is markedly controlled by the non obvious choice of the governing model. Of course, with an appropriate choice of the constitutive parameters, it is possible to obtain the same value of T_{cycle} with different models (one example is reported in Fig. 5).

5. Additional phenomena controlling the recurrence time: the thermal pressurization of pore fluids

Ample evidence has been discussed to demonstrate that fluid flow and/or pore pressure evolution can affect earthquake ruptures (Hubbert and Rubey, 1959; Miller et al., 1996; Yamashita, 1998; Shapiro et al.,

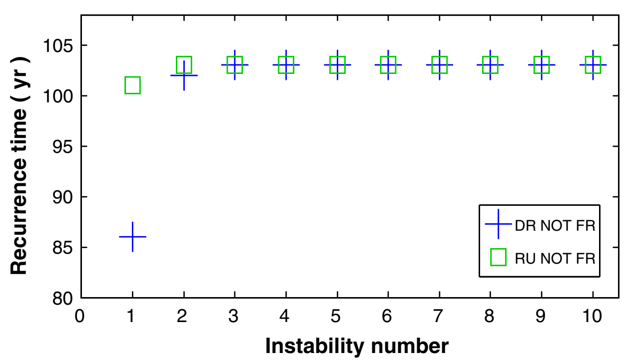

Fig. 5. Comparable T_{cycle} (approximately 123 years) obtained by properly tuning the constitutive parameters of the DR and RD governing models in not frozen conditions. To obtain this result we adopted the following values: $a=0.007$, $b=0.016$, $L=1.5\times10^{-2}$ m for the DR law and $a=0.004$, $b=0.013$, $L=1.0\times10^{-2}$ m for the RD law, respectively.

2003). In the source physics a prominent role is played by the thermal pressurization (TP henceforth) of the pore fluids; the frictional heat produced during the coseismic sliding causes an expansion of the fluids permeating the fault zone. The host rock matrix cannot deform so quickly to accommodate such a volume expansion and therefore it pressurizes the fluids, which are squeezed out of the fault (e.g., Lachenbruch, 1980).

The TP mechanism can play a very important role in determining the recurrence time of earthquakes; a typical example is reported in Fig. 5, where we compare a perfectly dry fault to a wet fault with TP. In the latter case the governing law is a modification of the classical DR model (see Eq. (40) in Bizzarri, 2011a and references cited therein). In this case the effective normal stress varies through time, since $\sigma_n^{eff}(t)=\sigma_n-p_{fluid}(t)$ (where σ_n is of tectonic origin and p_{fluid} is the pore fluid pressure, expressed as in Eq. (4) of Bizzarri, 2010). This variation causes in turn a modification to the frictional resistance of the fault (because $\tau=\mu\sigma_n^{eff}$, μ being the coefficient of friction) and a different evolution of the state variable.

Our results also confirm the findings by Mitsui and Hirahara (2009) that the pore fluid migration increases the recurrence interval of the instability events; for the parameters adopted here T_{cycle} increases by nearly 120% (from 138 years in the reference configuration to 165 years when TP is considered). This is basically due to the fact that TP also enhances the decelerating phase subsequent to an instability event, causing the system to reach a state having both the residual stress and the slip velocity lower than in the reference case (Fig. 6). This ultimately implies that the slider has to endure a more longer recovery phase (the inter-seismic fault restrengthening) before it undergoes the next slip failure (Bizzarri, 2010).

To summarize, we have seen that the inclusion of TP mechanism, can dramatically change the value of the earthquake recurrence time, as it occurs when we change the governing model for a dry fault (see Section 4).

6. The effects of wear

One of the prominent parameters in the TP model is the size of the slipping zone, $2w$, where the maximum deformation is concentrated (Bizzarri, 2009 and references cited therein). Some geological evidence suggests that $2w$ can be spatially variable even within the same fault structure (e.g., Rathbun and Marone, 2010). Moreover, there are indications from faults in mines, at outcrops and in laboratory specimens that wear processes occurring during brittle faulting cause the slipping zone to enlarge (Hull, 1988; Marrett and Allmendinger, 1990). Here, in agreement with Power et al. (1988), Robertson (1983) and Bizzarri (2010) we consider a linear variation of $2w$:

$$w(t) = Cu(t) \qquad (10)$$

where C being a dimensionless constant. Physically, this widening model assumes that the slipping zone thickness of natural faults depends on the accumulated slip because the micro-asperities that must be broken during sliding also depend on u. Since the displacement is controlled by the fault rheology, $2w$ also depends on the rheological properties of the sliding interface.

The results pertaining to models including wear evolution are reported in Fig. 7, where different values of the constant C of Eq. (10) have been assumed. Indeed, from Fig. 7a it is clear that, as long as $2w$ increases, the variations in σ_n^{eff} during the coseismic slip failures continuously decrease. With TP and constant $2w$ (red lines in Fig. 7a) the coseismic variations of σ_n^{eff} are roughly equal to 12 MPa (40% of ${\sigma_n^{eff}}_0$), while for varying $2w$ with $C=0.05$, after 1380 years we have $\Delta\sigma_n^{eff}$~4 MPa (13% of ${\sigma_n^{eff}}_0$). More interestingly for the present matter, we can see that the evolution of the slipping zone significantly changes the duration of the seismic cycle. To quantify this, we report in Fig. 7b

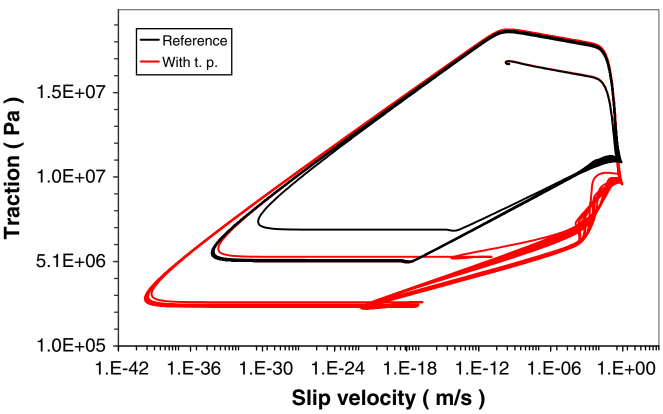

Fig. 6. Comparison between a dry (black curve) and wet fault with thermal pressurization (TP) of pore fluids (red curve). The adopted parameters are those of Table 1; in the latter case the additional parameters are: $T_0=100$ °C, $c=3\times10^6$ J/(m^3 °C) and $\kappa=1\times10^{-6}$ m^2/s (as in Fig. 3) and $\chi=1\times10^{-6}$ m^2/s, $\omega=0.4$ m^2/s, $\gamma=0.5$, $2w=1.4$ mm. (For interpretation of the references to color in this figure legend, the reader is referred to the web version of this article.)
Modified from Bizzarri (2010).

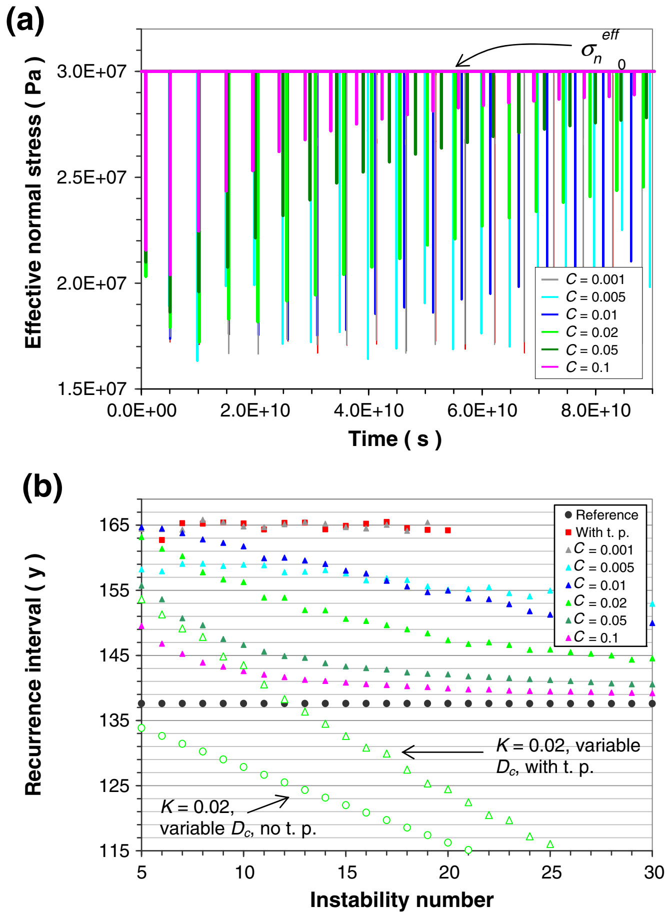

Fig. 7. Results pertaining to wet fault where TP is active and where wear evolution is also considered (see Eq. (10)). (a) Time evolution of the effective normal stress. (b) Resulting recurrence times. For comparison, we also include the reference case of a dry fault (black circles) and a wet fault with TP, but constant $2w$ (i.e., without wear effects). As for Fig. 4, T_{cycle} is computed in all cases starting from the 5th instability event, in order to avoid possible effects of the initial transient stage of the system.
Modified from Bizzarri (2010).

the estimated values of T_{cycle} for the different values of C as a function of subsequent instability events. Cases of a dry fault (black circles) and fluid-saturated fault, but with constant $2w$ (red squares) exhibit constant recurrence times, in that the system enters the limiting cycle (as already discussed in Section 2.4). This is also the case when $C \leq 0.001$, i.e., when wear processes are negligible. On the contrary, when wear is significant, we observe from Fig. 2d a continuous change in T_{cycle}, because the limiting reference cycle is not reached by the system in these cases. We emphasize that as long as $2w$ increases the pore fluid pressure variation is smaller and correspondently T_{cycle} decreases.

Therefore, we have shown here that the wear processes can significantly alter the inter-event times. In this case the system does not necessarily enter the limiting cycle and therefore, strictly speaking, the meaning of characteristic earthquake and recurrence time becomes somehow meaningless. Remarkably, this complicates the predictability of a subsequent earthquake, even in the idealized case of an isolated seismogenic fault.

7. The importance of the hydraulic properties and their evolution

In addition to the thickness of the slipping zone, $2w$ (considered in Section 6), the parameter of pivotal importance for fluid-infiltrated fault is the hydraulic diffusivity ω, which is defined as it follows:

$$\omega = \frac{K}{\eta_{fluid}\beta_{fluid}\Phi} \tag{11}$$

where K is the permeability of the medium, η_{fluid} is the dynamic viscosity of the fluid, β_{fluid} is its isothermal coefficient of compressibility and Φ is the porosity (e.g., Andrews, 2002). In general, β_{fluid} – which is defined as the inverse of the bulk modulus of elasticity of the fluid; namely: $\beta_{fluid} = \frac{1}{\rho_{fluid}}\frac{\partial\rho_{fluid}}{\partial p_{fluid}}|_{T=const}$, where ρ_{fluid} is the cubic mass density of the fluid and partial derivatives are calculated for constant temperature (Batchelor, 1967) – depends on the confining pressure and on the temperature (see Lachenbruch, 1980, his Fig. 1, and references cited therein; see also Garagash and Rudnicki, 2003). This dependence is non linear and an analytical, quantitative interpretation of the reported data – which is necessary in order to include these variations in our model – is presently missed. Also the dynamic fluid viscosity can change due to temperature variations. If the fluid is pure water, an empirical description of this variation is expressed by the following relation: $\eta_{fluid} = A10^{\frac{B}{T-C}}$, where the temperature T is in K, $A = 2.414 \times 10^{-5}$ Pa s, $B = 247.8$ K and $C = 140$ K (see Seeton, 2006 for a review). Even if we assume constant values of β_{fluid} and η_{fluid} the hydraulic diffusivity can change through time (thus exhibiting an implicit time dependence) due to temporal variations of porosity and permeability.

7.1. Porosity evolution

The porosity of a porous material (rock or sediment) is the dimensionless ratio between the current fraction of voids (pore volume; V_{voids}) with respect to the total volume (V_{tot}) of the material: $\Phi = \frac{V_{voids}}{V_{tot}}$. By definition, Φ (sometime indicated with the symbol n) fails in [0,1]; $\Phi < 0.01$ for solid granite and $\Phi > 0.5$ for clay (e.g., Paterson and Wong, 2005). Fault zone porosity is expected to change during a coseismic process due to the formation of the new cracks, changes to ineffective (or isolated) to effective (or connected) porosity (rearrangement of the interconnection chains between existing voids), grain size comminution, gouge evolution, etc. The time variations of Φ ultimately accounts for both frictional dilatancy ($\dot{\Phi} > 0$) and ductile compaction ($\dot{\Phi} < 0$). As comprehensively discussed by Bizzarri (2009), in the literature several analytical expressions of the time evolution of the porosity have been introduced; in this study we adopt the widely used model proposed by Sleep (1995; see also Segall and Rice, 1995), which is based on the critical state concept in soil mechanics, postulating the existence of a steady state porosity. In particular, Φ is assumed to be directly controlled by the evolution of the state variable Ψ:

$$\Phi(t) = \Phi_* - \varepsilon_{SR}\ln\left(\frac{\Psi v_*}{L_{SR}}\right) \tag{12}$$

where Φ_* is a reference value for porosity and ε_{SR} is a sensitivity parameter (or dilatancy coefficient, roughly ranging between 5×10^{-5} and 3×10^{-4}; see Samuelson et al., 2009), which controls the amount of variation of Φ and which physically represents a measure of porosity changes caused by velocity variations (namely is: $\varepsilon_{SR} = \Delta\Phi/\Delta\ln(v)$). We assume here the same value of Φ_* adopted in previous studies (Andrews, 2002; Bizzarri and Cocco, 2006; Mitsui and Cocco, 2010). L_{SR} is a characteristic scale length for the time evolution of Φ; laboratory experiments by Marone et al. (1990) indicate that in response to steps in slip velocity the porosity evolves toward a new steady state over a distance comparable to the evolution distance for the friction resistance (L). It is worth mentioning that the evolution law (12) refers to inelastic changes on pore volume (in other words the quantity Φ in Eq. (12) should be regarded as the plastic component of porosity). The inclusion of a thermoelastic part, due to changes of pore pressure and temperature with respect to the initial conditions, can eventually increase the effect of the plastic component of the porosity (Segall and Rice, 1995).

7.2. Permeability evolution

The permeability physically represents a measure of the ability of a porous rock or a unconsolidated material to transmit fluids. It is often expressed through the hydraulic conductivity (κ) via $K = \kappa\frac{\eta_{fluid}}{\rho_{fluid}g}$, where g is the acceleration of gravity. In the special case of a single-phase porous material the permeability is an intensive property, i.e., it is a function of the material structure only and, as such, it is scale invariant (it does not depend on the amount of the porous material or on the system size). This is not the case in geological systems, where larger system sizes generally have larger conduits for fluid flow. Permeability enters as a part of the proportionality constant in the Darcy's law, expressing the volumetric flow rate of the fluid per unit area (q_ζ, also named Darcy's velocity) as a function of the pressure gradient (in one dimension (ζ) we have: $q_\zeta = -\frac{K}{\eta_{fluid}}\frac{d}{d\zeta}p_{fluid}$). The estimation of the permeability is of pivotal importance in many areas of Earth sciences, TP mechanism, magma degassing, hydrocarbon recovery, etc.

Unfortunately, though permeability measurements were performed in different rock types (e.g., Zhang et al., 1999; Wibberley and Shimamoto, 2003), because of technical difficulties, this fundamental parameter is difficult to estimate at seismic deformation conditions (i.e., slip rate of 1 m/s).

Local variations of the rock permeability have been inferred from observations of natural faults and from laboratory samples (Jourde et al., 2002). One possibility, essentially due to Rice (1992), postulates an explicit dependence of K on the effective normal stress:

$$K(t) = K_* e^{-\frac{\sigma_n^{eff}(t)}{\sigma_{n*}}} \tag{13}$$

in which K_* and σ_{n*} are reference values of permeability and normal stress, respectively.

Another possibility for the evolution of K we consider consists in the Kozeny–Carman's model, which directly relates the permeability to the porosity (Kozeny, 1927; Carman, 1937). This amenable link between media properties and flow resistance inside pore channels suffers from the intrinsic difficulty of evaluating in detail the spatial shape of the channels and their distribution. Among the large number of the formulations of the Kozeny–Carman's relation (see also Costa, 2006 for a discussion) we adopt here the following equation:

$$K(t) = K_{KC}\frac{(\Phi(t))^3}{(1-\Phi(t))^2}(D(t))^2 \quad (14)$$

K_{KC} being a dimensionless parameter (which generally depends on the material; see Costa, 2006 and references cited therein) and D the (average) diameter of the grains (ranging between 4×10^{-5} m and 1×10^{-4} m; see Niemeijer et al., 2010). The explicit time dependence of D in Eq. (14) accounts for possible gouge refinement and fragmentation; in the present approach, however, we will simply consider a constant diameter $D = D_0$ (therefore Eq. (14) is equivalent to the relation $K(t) = K'_{KC}\frac{(\Phi(t))^3}{(1-\Phi(t))^2}$, with $K'_{KC} \equiv K_{KC}D_0^2$). We do not want overemphasize that in this case only a time variable porosity causes temporal changes in K.

7.3. Numerical results

As pointed out by Bizzarri (2012b), the time variations of hydraulic diffusivity only due to porosity changes (through Eq. (12)) do not markedly affect the earthquake recurrence (cycle time), the traction evolution and the thermal history of the fault, regardless the values of the two free parameters ε_{SR} and L_{SR}. On the contrary, the time variations of the permeability alone, in agreement to the Rice (1992)'s model (Eq. (13)) cause large increases in ω that tend to anticipate an instability and therefore tend to reduce the seismic cycle, as it emerges from Fig. 8.

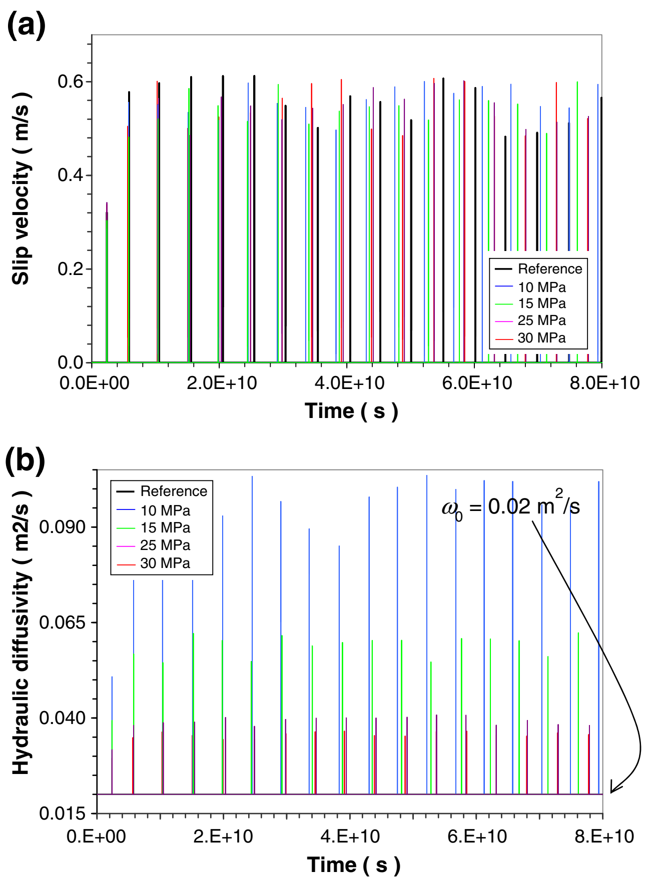

Fig. 8. Results of a wet fault with TP and variations of the hydraulic diffusivity ω only due to variations of permeability K (see Eq. (13)). (a) Time evolution of the slip velocity. (b) Time evolution of the resulting ω, with the reference (initial) value indicated. Black lines refer to a reference case having constant ω and $\sigma_{n^*} = 30$ MPa. The values reported in the legends are the different values of the parameter σ_{n^*} in Eq. (13). The adopted parameters are those of Fig. 6, except $a = 0.01$, $2w = 2.2$ mm; $K_* = 1.35914\times10^{-16}$ m^2 (so that $K(t=0) = 5\times10^{-17}$ m^2, as in Fig. 6).
Modified from Bizzarri (2010).

In Fig. 9 we report the results pertaining the incorporation of the variations of both porosity and permeability (thought the implementation of the Kozeny–Carman's model; Eq. (14)). In this case we can see significant reductions in the seismic cycle with respect to the reference configuration having constant properties. Indeed, the time variations of the pore fluid pressure in the correspondence of the dynamic events are smaller in the case of the Kozeny–Caraman's model and this ultimately leads to a reduction of the frictional resistance (we recall here that $\tau = \mu(\sigma_n - p_{fluid})$) and this causes an anticipation of the occurrence of earthquakes (Fig. 9a). Indeed, by looking at Fig. 9b, we see that the time evolution of the porosity causes a small increase in the hydraulic diffusivity during the intersesimic period and a more relevant decrease in the correspondence of the instability events. Conversely, the evolution of K tends to do the opposite (see also Fig. 8b). The inclusion of the Kozeny–Caraman's model shows that the evolution of K dominates that of Φ.

8. Temperature-dependence of constitutive parameters

As already discussed in Bizzarri (2011a), the two constitutive parameters appearing in the rate- and state-dependent friction laws which basically controls the level of instability of a fault are a and b. Physically, they account for the effects of thermally-activated exponential creep occurring at the microscopic level and govern the macroscopic processes of earthquakes, as well as the formation of faults by strain rate localization. There are several evidences suggesting that they can depend explicitly on the temperature (Blanpied et al.,

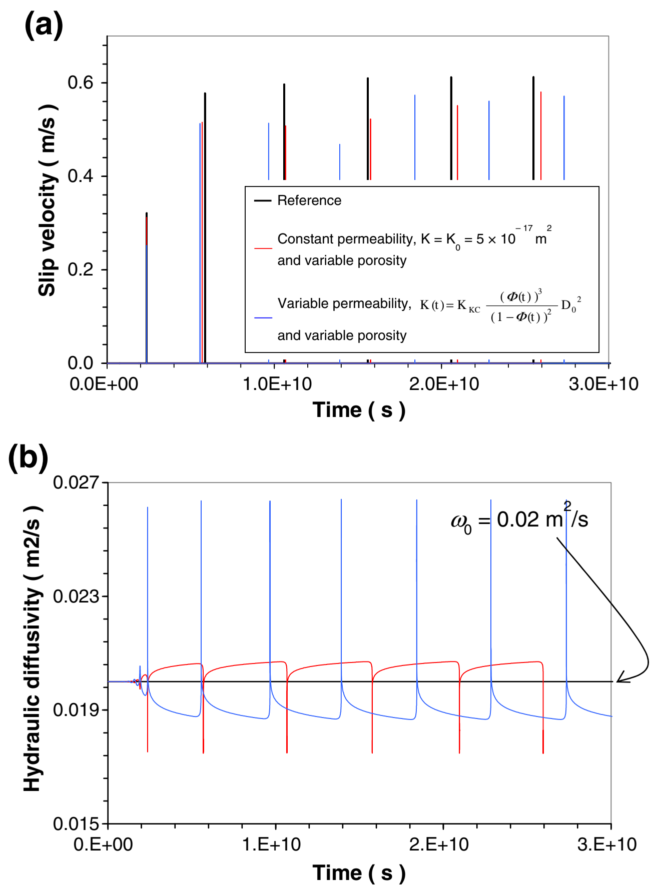

Fig. 9. The same as in Fig. 8, but the variations of ω are due to both variations of K and porosity Φ (see Eqs. (12) and (14)). In this case: $K_{KC} = 3.042\times10^{-4}$ (so that $K(t=0) = 5\times10^{-17}$ m^2); $D_0 = 0.1$ mm, $\Phi_0 \equiv \Phi(t=0) = 0.025$.
Modified from Bizzarri (2012b).

1998; Nakatani, 2001), leading to a temperature-dependent rheology. Here we consider a linear dependence of the constitutive parameter a on the absolute temperature T:

$$a = \frac{k_B}{V_a h} T \qquad (15)$$

where k_B is the Boltzmann's constant ($k_B = 1.38 \times 10^{-23}$ J/K), V_a is the activation volume ($V_a = Q\Omega k_B/R$, where Q is a dimensionless constant, Ω is the effective molecular volume and R is the gas constant; Gordon, 1967; Sleep, 1997), h is the hardness (within the framework of the classical adhesion theory, we have: $h = A_m \sigma_n / A_{ac}$, where A_m and A_{ac} are the nominal and real contact area, respectively, and σ_n is the macroscopic normal stress; Holm, 1946). We will emphasize that T is not an experimental, externally-imposed condition, but it is due to the frictional heating.

A typical evolution of the parameter a following Eq. (15) is reported in Fig. 10a. In Fig. 10b–d we report the comparison between a reference case with constant a (black curves) and a model with time-variable a (red curves). The implicit time dependence of a causes temporal changes in the two basic parameters controlling the degree of instability of a fault:

$$\bar{\kappa} = \frac{k_{cr}}{k} = \frac{B - A}{kL} \qquad (16)$$

and

$$\beta = \frac{B}{A} \qquad (17)$$

in which $A \equiv a\sigma_n^{eff}$ and $B \equiv b\sigma_n^{eff}$. The more $\bar{\kappa}$ and β exceed 1 the more unstable the fault is, i.e., peaks in v and the stress releases are larger. In the simulations presented in Fig. 10b–d the effective normal stress is temporally constant, so that β equals b/a and it has been interpreted as the relative efficiency of the grain lattice in aiding frictional sliding versus compaction (Sleep, 1997). The conditions guaranteeing an unstable behavior ($\bar{\kappa} > 1$ and $\beta > 1$) are not necessarily satisfied when b is kept constant ($b(t) = b_0$, $\forall\, t \geq 0$) and only a varies though time. Both configurations start from the same initial conditions (Fig. 10c), defining a velocity weakening regime ($\beta > 1$), but as long as the system evolves the two cases diverge. In fact, we can now observe that the peaks in v are significantly reduced, roughly by a factor of 10 (Fig. 10b); remarkably, this reduction can solve the physical paradox of extremely large slip velocities, often resulting from numerical experiments (Noda et al., 2009). Moreover, this has its counterpart in the diminution of the developed slip, suggesting (in a more complex 3-D fault model) a decrease of the size (i.e., the seismic moment, M_0) of the earthquake events.

From Fig. 10c it is apparent that the stress released after each instability is reduced with respect to the reference configurations, while the minima of the slip velocity after the dynamic event are larger. This implies that interseismic fault restrengthening is faster in the case with variable a and therefore the seismic cycle is shorter in this case; notably, the cycle time is significantly reduced (se also Fig. 10b) from a value of 51 years to 25 years when a is varying. Indeed, we can see from Fig. 10d that when a varies the system can spontaneously reach the conditionally stable regime ($\bar{\kappa} < 1$; see Eq. (16) and Scholz, 2002) and even the velocity strengthening regime ($\beta < 1$; see Eq. (17)).

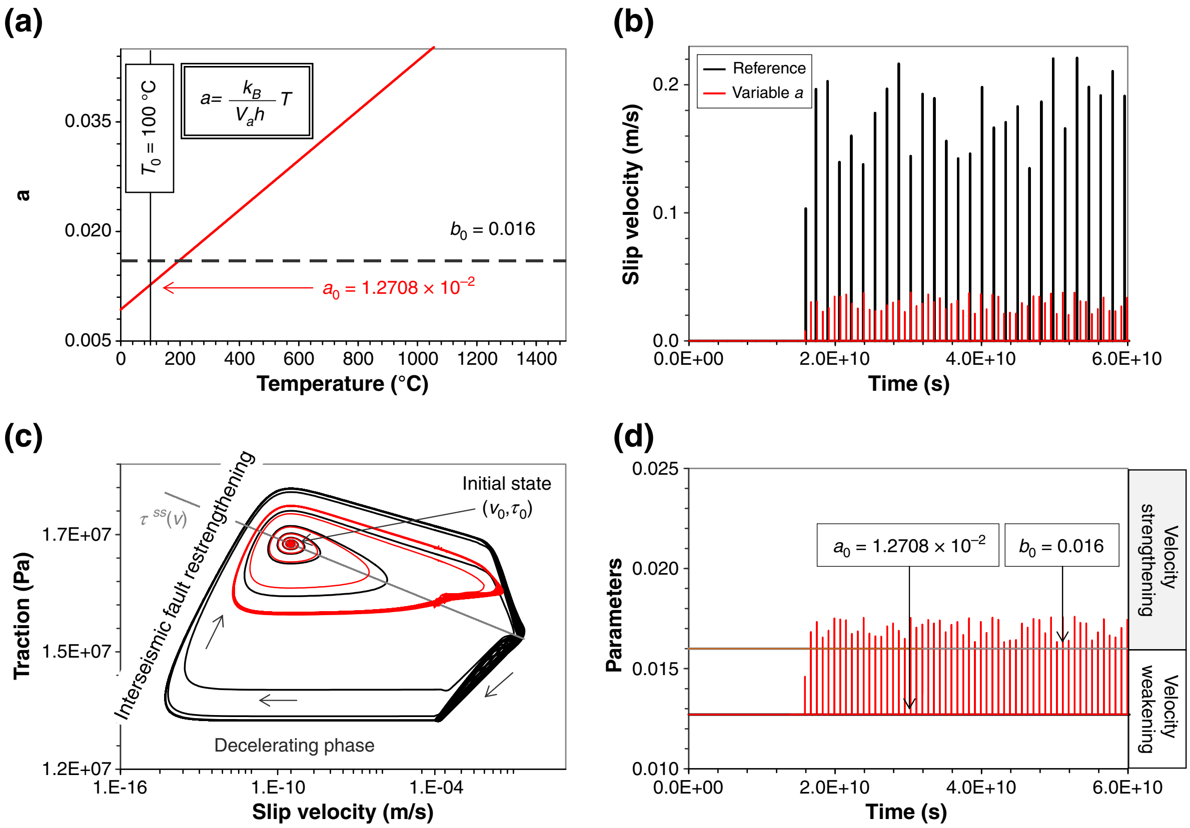

Fig. 10. (a) Evolution of the parameter a with the temperature, in agreement with Eq. (15). (b)–(d) Comparison between the reference model, with constant a (black curves), and a model where the parameter a is varying (red curves). (b) Time histories of slip velocity; note the reduction of peaks in slip velocity roughly from 0.2 m/s to 0.02 m/s. (c) Phase portrait (i.e., traction vs. slip velocity). The steady state traction for the reference configuration, defined as $\tau^{ss}(v) = \mu_* \sigma_n^{eff} + (B - A)\ln(\frac{v_*}{v})$, is reported in gray. (d) Time evolution of the constitutive parameters a and b. The adopted parameters are those of Fig. 6, except for $a_0 \equiv a(t=0)$ (which is reported in panel (a)), $L = 7$ mm and $2w = 1.5$ mm. The additional parameters are: $V_a = (0.37\ \text{nm})^3$ and $h = 8$ GPa. (For interpretation of the references to color in this figure legend, the reader is referred to the web version of this article.) Modified from Bizzarri (2011b).

As an overall conclusion we can state that a temperature-dependent rheology described by Eq. (15) has relevant consequences in the dynamics of the fault and in particular influence the value of the cycle time. This conclusion also agrees with the results discussed in Section 4, where we have shown that a rate-, state- and temperature-dependent friction exhibits shorter recurrence times with respect to a classical rate- and state-dependent governing model (see Fig. 4).

9. Discussion

As pointed out by Allen (2007), the great challenge of natural hazard reduction, and in particular of the earthquake hazard mitigation, is represented by the relative infrequency of large events (i.e., the long recurrence interval of these events), which provide only a limited data set for the study of the impacts of these events on the modern cities. The concept of the cyclicity of the earthquake ruptures is the theoretical assumption which founded the seismic gap method (Kelleher et al., 1973) of earthquake forecasting (the utility of which remains a matter of debate; see Allen, 2007 and references cited therein). If we assume that a fault segment fails in a quasi-periodic series of characteristic earthquakes (CEs), then the recurrence interval between the events can be estimated. This belief is in line with the official earthquake prediction of the US National Earthquake Prediction Evaluation Council (Shearer, 1985; Jackson and Kagan, 2006). The seismic gap method reported a great success in occasion of the 1923 Kanto earthquake, the Nankaido earthquakes of 1944 and 1946 (Aki, 1980; Nishenko, 1989), as well as the 1968 Tokachi-Oki, 1969 Kuriles and 1971 central Kamchatka earthquakes (Fedotov, 1965; Mogi, 1985). On the other hand, it is worth mentioning that, based on the evidence of recurrent earthquakes, Bakun and Lindh (1985) predicted that the next earthquake at Parkfield, California, was due in 1988 with a 95% confidence that it would occur before 1993. However, a M 6.0 earthquake did occur on the Parkfield segment of the San Andreas, but not until September 28, 2004 (Langbein et al., 2005 had then shown that it was of the same magnitude of the previous event, but the characteristics of its rupture were different). On the other hand, it should be mentioned that the concept of CE has been often criticized, in that some authors claim that it is a statistical artifact (e.g., Kagan, 1996; Kagan et al., in press). Moreover, Kagan and Jackson (1995) show that the seismic gap pattern could be rejected with the 95% confidence level.

As pointed out by Molchan et al. (1997), the time behavior of a CE is treated as a nonpoissonian renewal process. In this framework, the recurrence interval T_{cycle} makes it possible to expresses the probability p of occurrence of earthquakes with magnitude exceeding M in a given exposure time (e.g., Panza et al., 2011):

$$p(t) = 1 - e^{-\frac{t}{T_{cycle}}}. \tag{18}$$

It is evident from Eq. (18) that an adequate understanding of the rate of the complexity of the earthquake recurrence is a key issue in seismic hazard assessment. Unfortunately, the prediction of T_{cycle} for a given seismic source is not still solved unequivocally. Nevertheless, the concept of recurrence time has practical implications, since it significantly affects ground shaking probability estimates and the related hazard maps, as shown by Zuccolo et al. (2011); the technical rules of building construction in Italy (Norme tecniche di costruzione, 2008) are presently based upon the concept of T_{cycle} (see Table 1 therein). It is worth mentioning that in Italy we are still far from the development of "dynamic, intelligent" buildings, integrated with early-warning systems, which can change their mechanical properties within a few seconds to better withstand ground motion (active or semi-active systems), as some engineering companies in Japan are developing (Housner et al., 1997), and buildings equipped with passive systems (base isolation, viscoleastic dampers, etc.).

Several attempts have been made in order to relate T_{cycle} to the magnitude of an event. For small earthquakes Nadeau and Johnson (1998) suggest the following scaling relation:

$$T_{cycle} \propto M_0^{1/6} \tag{19}$$

which has been also extended from the repeating earthquakes along the Parkfield segment of the San Andreas fault to other tectonic environments (Chen et al., 2007). This empirical relation requires that either the stress drop, $\Delta\tau$, and the long term slip velocity accommodated by the fault segment, v_L, or both can have some dependence on M_0. In Section 6 we have clearly demonstrated that the stress release can change during the entire life of the fault, depending on the cumulated slip. In the idealized situation where $\Delta\tau$ and v_L are constant, Beeler et al. (2001) propose the relation:

$$T_{cycle} = \frac{\Delta\tau^{2/3}}{1.81\, G v_L} M_0^{1/3} \tag{20}$$

where G is the shear modulus. Basically, Eq. (20) indicates that $T_{cycle} \propto M_0^{1/3}$. Indeed, we know that the contact time-dependent fault healing effects (e.g., Dieterich, 1972; Beeler et al., 1994; Marone et al., 1995) can change the strength of a fault and therefore the critical tectonic load required to reach the yield point causing each instability (so that the amenable relation $T_{cycle} \propto v_{load}$, valid for a CE, no longer hold). On the other hand, if $\Delta\tau$ is constant, to have the behavior of Eqs. (19) and (20) indicates that it is necessary to have $v_{load} \propto M_0^{1/6}$, i.e., the ratio of the tectonic load released seismically and that released aseismically is size-dependent, but this is under debate in the seismological community (e.g., Anooshehpoor and Brune, 2001).

At a more fundamental level, the ubiquitous, epistemic uncertainties related to the state of that source (in terms of sliding speed and mainly of stress) and those related to its governing equations (describing deterministically the dissipative physico-chemical process occurring therein) dramatically complicate the prediction of the recurrence interval (Gabrielov and Keilis-Borok, 1983; Gabrielov and Newman, 1994; Kagan, 1994; Kanamori, 2003). Moreover, the frequent inaccessibility of a fault zone to direct measurements and the heterogeneous state of the Earth further impose additional difficulties (e.g., Geller et al., 1997). Measurements of the crustal deformations near a given fault obtained from GPS and InSAR methods can help us in determining the rate at which that fault is loaded. On the other hand, laboratory experiments conducted in realistic conditions and theoretical models of faulting illuminate us about the possible governing law for faults.

It is well known that the amplitude of the ground motions is physically related to the seismic moment of an earthquake. In engineering analysis, in addition to the strong motion duration, one of the most universal adopted parameters is the peak ground acceleration (PGA) combined by a specific spectral shape (in this sense this engineering PGA is not necessarily identical to the seismological PGA measured in a real earthquake). We recall here that the use of PGA is disputable (see also Klügel et al., 2009), since it is not appropriate for tall buildings – for which the use of the peak ground velocity (PGV) is preferable, having high natural periods – and because PGA is not always closely related to the observed damage (Panza et al., 2011, 2012; Zuccolo et al., 2011; see also Kossobokov and Nekrasova, 2012 and references cited therein), contrary to the intensity (Klügel et al., 2009). On the other hand, it has become increasingly evident that seismic hazard maps generated by the Global Seismic Hazard Assessment Program (GSHAP; www.seismo.ethz.ch/static/GSHAP), in which orange and red colors indicate elevated PGA with 10% probability of exceedance in 50 years corresponding to a return period of 475 years, do not correctly give the seismic hazard, especially for disastrous earthquakes with $M \in [6.9, 8.6]$ (Wyss et al., 2012; Kossobokov and Nekrasova, 2012; see also Zuccolo et al., 2011).

Indeed, the relevant inconsistencies emerging from the systematic and quantitative comparison between the GSHAP maps and the factual effects under strong earthquakes led Kossobokov and Nekrasova (2012) to formulate a strict verdict of useless for this kind of probabilistic product in the framework of any type of evaluation of the seismic hazard (it has been found that GSHAP fails both in predicting expected ground shaking and in describing past seismicity). Having in mind the substantial differences existing between risk and hazard, risk reduction and hazard mitigation (Panza et al., 2011), it is clear that standard hazard maps (which basically provide the basis for the risk estimates), as well as engineering practices, have to be critically revisited and scrutinized (Wyss et al., 2012). This led to the formulation, at regional and local scales, of the so-called time-dependent neo-deterministic seismic hazard analysis (NDSHA), which produces a set of seismic scenarios (i.e., synthetic ground motion signals) based upon the physics of the earthquake source and wave propagation models (Panza et al., 2001; Zuccolo et al., 2011 and referenced cited therein).

Moreover, although the locations of most of the major active faults that generate large earthquakes are known, unrecognized active faults or unrecognized styles of deformation are likely to exist in the Earth and it is problematic to quantitatively treat such uncertainties. At the same time, we cannot exclude that the major changes in the tectonics which are now occurring and which cause the rates of plate motion will not apply in the next thousand years. Both these uncertainties led Molnar (1979) to conclude that the historical record of seismicity from most regions is too short to allow an estimation of the frequency of occurrence of major earthquakes with much confidence. A typical example can be found in the M 9.0 Tohoku, Japan earthquake, which occurred in March 2011 in a region where only M 8.0 quakes were expected.

10. Conclusive remarks

In this paper we have discussed the various complications arising in the determination of the recurrence time of earthquake events. We adopt the simplest fault analog system, the one-degree-of-freedom mass–spring model (e.g. Gu et al., 1984), which makes us able to model the whole seismic cycle on a given fault structure in a computationally efficient way. The model adopted here is intentionally simple, because it disregards any possible complication arising from the presence of heterogeneities in the rheological properties of the fault system and from possible geometrical complexities. The results obtained with this kind of analog fault model can be regarded as a proxy of the true behavior of an extended seismogenic fault embedded in a continuous medium. Several studies show that the mass–spring analog model is able to capture the basic physics of the seismogenic fault and of the dissipative process occurring during its cycle (far of being exhaustive, see Rice and Gu, 1983; Gu et al., 1984; Tse and Rice, 1986; Boatwright and Cocco, 1996; Roy and Marone, 1996; Gomberg et al., 1997, 2000; Bizzarri, 2010, 2011a, 2012b).

We have shown that many different factors influence the determination of T_{cycle} (formally defined by Eq. (5)) which often makes this concept misleading or fruitless.

(1) Fault interactions and stress triggering phenomena (Section 3) probably are the most apparent causes of the complexity of the seismic sequences and of the spatial distribution of epicenters. Indeed, the stress redistribution arising from a causative fault can activate neighboring structures and induce new events (e.g., Gomberg et al., 1997) complicating the cyclicity of a CE.

(2) The analytical expression of the fault governing law, which describes the traction evolution during faulting and accounts for the different, and mutually interacting, physico-chemical dissipative processes (Bizzarri, 2009, 2011a), has serious consequences in the determination of T_{cycle}. We have shown is Section 4 that even if a single, isolated fault, starts from a given initial state **U**, the choice of the constitutive models dramatically affects the resulting recurrence time. Remarkably, this choice is not obvious and pertains to the epistemic uncertainties, intimately related to the seismic source physics. The challenging researches in this area, conducted both from a theoretical and an experimental approach, indubitably represent a prominent contribution in the framework of the deterministic description (i.e., physical forward modeling) of the earthquake failures, but we do not still have a definitive answer to this impelling question.

(3) A special role in the determination of the recurrence time is represented by thermal pressurization of pore fluids (e.g., Lachenbruch, 1980; see Section 5). Indeed, it has been proved that TP affects not only the coseismic phase of the rupture (Andrews, 2002; Bizzarri and Cocco, 2006), but also T_{cycle} (Mitsui and Hirahara, 2009). In particular, we can conclude that fluid-permeated faults, if the slipping zone thickness is of millimeter size, systematically exhibit longer recurrence intervals compared to dry faults or structure where TP is not active.

(4) In Section 6 we have shown that wear processes, resulting in the widening of the slipping zone thickness, further complicate the results obtained with TP. In this case T_{cycle} is no longer a properly-defined quantity, in that it depends on the total cumulative slip at a given time. In this case, the concept of recurrence interval becomes even misleading (Bizzarri, 2010), because we cannot predict a priori the next occurrence of a coseismic slip failure.

(5) During seismic faulting the variations of the hydraulic properties can also occur, as discussed in Section 7. In particular, the permeability of the fault zone and its porosity can evolve through time (Mitsui and Cocco, 2010; Bizzarri, 2012b). This further complicates the determination of the seismic cycle time, which tends to be reduced with respect to a reference configuration with constant permeability and porosity.

(6) The Arrhenious nature of the so-called direct effect in the framework of the rate- and state-dependent friction laws (which expresses the dependence of the frictional resistance on the slip velocity through the constitutive parameter a; see for instance Gu et al., 1984) suggests a temperature-dependent rheology of fault structures (Blanpied et al., 1998; Nakatani, 2001). In Section 8 we have shown that the interseismic fault restrengthening is faster in the case of variable a and that therefore the seismic cycle is shorter in this case.

Moreover, it should be noted that in addition to the processes considered in the present study, also some other possible mechanisms (eventually still unknown) can contribute to affect the recurrence time.

The conclusions discussed in this work represent another way to demonstrate that earthquake recurrence does not follow an ergodic stochastic process, as previously discussed by Klügel (2005, 2008, 2011). They also can contribute to the vigorous debate concerning the concepts of characteristic earthquake and recurrence time within a physical modeling of earthquake events. Indeed, we demonstrate that the concept of recurrence time for earthquakes has severe limitations and is not generally applicable. This puts under question the current practice of building codes that are essentially based on PSHA, which in turn rely on this concept (either the Gutenberg–Richter low or the characteristic magnitudes). The currently widely used assumptions of cyclicity (recurrence) of earthquakes are only valid under very stable seismo-tectonic conditions and for isolated fault conditions with respect to the dominating active faults in a region. Such conditions exist only for geologically very short time periods (the assumption of invariance of boundary conditions and (at least) of only minimal changes of initial conditions do not hold for long time periods) and in seismo-tectonic settings with dominating fault systems (for instance in subduction zones). Moreover, the analysis presented here confirms that the currently in use methods of PSHA, and especially the use of probabilistic seismic hazard maps as the basis of building codes, cannot be endorsed as the basis methodology for seismic risk reduction. This is especially true in the case of cultural heritage buildings and critical structure, such as nuclear power plants, where it is necessary to consider extremely long time intervals.

Although earthquake engineering and seismology are relatively juvenile disciplines the average chance of being killed in an earthquake is a factor of 3 less than it was in 1900 (by the way, since 1900, 12 earthquakes in China, Pakistan, Iran, Indonesia, Japan, Italy and Peru caused more than 50,000 fatalities; Allen, 2007). The continuous reduction of this factor is at the same time a challenge and a motivation for the near future, which should be pursued by combining probabilistic and deterministic methodologies, as well as precursory studies.

Acknowledgments

The author wishes to thank G. F. Panza for fruitful, early discussions on the concept of the recurrence time and GSHAP maps. P. Crupi is kindly acknowledged for the assistance in the preparation of some figures. The author also thanks the Editor and two anonymous referees for stimulating comments and useful suggestions.

References

Aki, K., 1980. Possibilities of seismology in the 1980s. Bulletin of the Seismological Society of America 70, 1969–1976.

Allen, R. M., 2007. Earthquake hazard mitigation: New directions and opportunities. In Treatise on Geophysics (G. Schubert Ed.). 4 — Earthquake seismology (H. Kanamori Ed.). 607–648. Elsevier. http://dx.doi.org/10.1016/B978-044452748-6/00083-3.

Andrews, D.J., 2002. A fault constitutive relation accounting for thermal pressurization of pore fluid. Journal of Geophysical Research 107 (B12), 2363. http://dx.doi.org/10.1029/2002JB001942.

Anooshehpoor, A., Brune, J.N., 2001. Quasi-static slip rate shielding by locked and creeping zones as an explanation for small repeating earthquakes at Parkfield. Bulletin of the Seismological Society of America 91 (2), 401–403.

Bak, P., Tang, C., Wiesenfeld, K., 1987. Self-organized criticality — an explanation of 1/F noise. Physical Review Letters 59 (4), 381–384. http://dx.doi.org/10.1103/PhysRevLett.59.381.

Bakun, W.H., Lindh, A.G., 1985. The Parkfield, California, earthquake prediction experiment. Science 229, 619–624.

Bakun, W.H., McEvilly, T.V., 1979. Earthquakes near Parkfield, California: comparing the 1934 and 1966 sequences. Science 205, 1375–1377.

Batchelor, G.H., 1967. An Introduction to Fluid Dynamics. Cambridge Univ. Press, New York . 615 pp.

Beeler, N.M., Tullis, T.E., Weeks, J.D., 1994. The roles of time and displacement in the evolution effect in rock friction. Geophysical Research Letters 21 (18), 1987–1990.

Beeler, N.M., Lockner, D.L., Hickman, S.H., 2001. A simple stick-slip model for repeating earthquakes and its implication for microearthquakes at Parkfield. Bulletin of the Seismological Society of America 91 (6), 1797–1804.

Belardinelli, M.E., Bizzarri, A., Cocco, M., 2003. Earthquake triggering by static and dynamic stress changes. Journal of Geophysical Research 108 (B3), 2135. http://dx.doi.org/10.1029/2002JB001779.

Bizzarri, A., 2009. What does control earthquake ruptures and dynamic faulting? A review of different competing mechanisms. Pure and Applied Geophysics 166 (5–7), 741–776. http://dx.doi.org/10.1007/s00024-009-0494-1.

Bizzarri, A., 2010. On the recurrence of earthquakes: Role of wear in brittle faulting. Geophysical Research Letters 37, L20315. http://dx.doi.org/10.1029/2010GL045480.

Bizzarri, A., 2011a. On the deterministic description of earthquakes. Reviews of Geophysics 49, RG3002. http://dx.doi.org/10.1029/2011RG000356.

Bizzarri, 2011b. Temperature variations of constitutive parameters can significantly affect the fault dynamics. Earth and Planetary Science Letters 306, 272–278. http://dx.doi.org/10.1016/j.epsl.2011.04.009.

Bizzarri, A., 2012a. Modeling repeated slip failures on faults governed by slip-weakening friction. Bulletin of the Seismological Society of America 102 (2), 812–821. http://dx.doi.org/10.1785/0120110141.

Bizzarri, A., 2012b. Effects of permeability and porosity evolution on simulated earthquakes. Journal of Structural Geology 38, 243–253. http://dx.doi.org/10.1016/j.jsg.2011.07.009.

Bizzarri, A., 2012c. Formulation of a fault governing law at high sliding speeds: Inferences from dynamic rupture models. Earth and Planetary Science Letters 355–356, 223–230. http://dx.doi.org/10.1016/j.epsl.2012.09.007.

Bizzarri, A., Belardinelli, M.E., 2008. Modelling instantaneous dynamic triggering in a 3-D fault system: application to the 2000 June South Iceland seismic sequence. Geophysical Journal International 173, 906–921. http://dx.doi.org/10.1111/j.1365-246X.2008.03765.x.

Bizzarri, A., Cocco, M., 2003. Slip-weakening behavior during the propagation of dynamic ruptures obeying rate- and state-dependent friction laws. Journal of Geophysical Research 108 (B8), 2373. http://dx.doi.org/10.1029/2002JB002198.

Bizzarri, A., Cocco, M., 2006. A thermal pressurization model for the spontaneous dynamic rupture propagation on a three-dimensional fault: 2. Traction evolution and dynamic parameters. Journal of Geophysical Research 111, B05304. http://dx.doi.org/10.1029/2005JB003864.

Bizzarri, A., Spudich, P., 2008. Effects of supershear rupture speed on the high-frequency content of *S* waves investigated using spontaneous dynamic rupture models and isochrone theory. Journal of Geophysical Research 113, B05304. http://dx.doi.org/10.1029/2007JB005146.

Bizzarri, A., Cocco, M., Andrews, D.J., Boschi, E., 2001. Solving the dynamic rupture problem with different numerical approaches and constitutive laws. Geophysical Journal International 144, 656–678.

Blanpied, M.L., Marone, C.J., Lockner, D.A., Byerlee, J.D., King, D.P., 1998. Quantitative measure of the variation in fault rheology due to fluid–rock interactions. Journal of Geophysical Research 103, 9691–9712.

Boatwright, J., Cocco, M., 1996. Frictional constraints on crustal faulting. Journal of Geophysical Research 101 (B6), 13895–13909. http://dx.doi.org/10.1029/96JB00405.

Burridge, R., Knopoff, L., 1967. Model and theoretical seismicity. Bulletin of the Seismological Society of America 57, 341–371.

Carlson, J.M., Langer, J.S., 1989a. Properties of earthquakes generated by fault dynamics. Physical Review Letters 62, 2632–2635. http://dx.doi.org/10.1103/PhysRevLett.62.2632.

Carlson, J.M., Langer, J.S., 1989b. A mechanical model of an earthquake fault. Physical Review A 40, 6470–6484. http://dx.doi.org/10.1103/PhysRevA.40.6470.

Carman, P., 1937. Fluid flow through a granular bed. Transactions of the Institution of Chemical Engineers 15, 150–167.

Chen, K.H., Nadeau, R.M., Rau, R.J., 2007. Towards a universal rule on the recurrence interval scaling of repeating earthquakes? Geophysical Research Letters 34. http://dx.doi.org/10.1029/2007GL030554.

Costa, A., 2006. Permeability-porosity relationship: a reexamination of the Kozeny–Carman equation based on a fractal pore-space geometry assumption. Geophysical Research Letters 33, L02318. http://dx.doi.org/10.1029/2005GL025134.

Cotton, F., Coutant, O., 1997. Dynamic stress variations due to shear faults in a plane-layered medium. Geophysical Journal International 128, 676–688.

Day, S.M., Dalguer, L.A., Lapusta, N., Liu, Y., 2005. Comparison of finite difference and boundary integral solutions to three-dimensional spontaneous rupture. Journal of Geophysical Research 110, B12307. http://dx.doi.org/10.1029/2005JB003813.

de Lorenzo, S., Loddo, M., 2010. Effect of frictional heating and thermal advection on pre-seismic sliding: a numerical simulation using a rate-, state- and temperature-dependent friction law. Journal of Geodynamics 49, 1–13. http://dx.doi.org/10.1016/j.jog.2009.07.001.

Dieterich, J.H., 1972. Time-dependent friction in rocks. Journal of Geophysical Research 77, 3690–3697.

Dieterich, J.H., 1978. Time-dependent friction and the mechanics of stick slip. Pure and Applied Geophysics 116, 790–806.

Fedotov, S.A., 1965. Regularities of distribution of strong earthquakes in Kamchatka, the Kuril Islands and northern Japan (in Russian). Akademia Nauk SSSR, Institut Fiziki Zemli Trudy, 36, pp. 66–93.

Findlay, A., 1911. The Phase Rule and its Applications, 3rd ed. Longmans, Green and Co.

Gabrielov, A.M., Keilis-Borok, V.I., 1983. Patterns of stress corrosion: geometry of the principal stresses. Pure and Applied Geophysics 121 (3), 477–494.

Gabrielov, A.M., Newman, W., 1994. Seismicity modelling and earthquake prediction: a review. Non-linear dynamics and predictability of geophysical phenomena: IUGG Geophysical monograph, 83.

Garagash, D.I., Rudnicki, J.W., 2003. Shear heating of a fluid-saturated slip-weakening dilatant fault zone, 1, limiting regimes. Journal of Geophysical Research 108 (B2), 2121. http://dx.doi.org/10.1029/2001JB001653.

Geller, R.J., Jackson, D.D., Kagan, Y.Y., Mulargia, F., 1997. Earthquakes cannot be predicted. Science 275, 1616–1617.

Gomberg, J., Blanpied, M.L., Beeler, N.M., 1997. Transient triggering of near and distant earthquakes. Bulletin of the Seismological Society of America 87, 294–309.

Gomberg, J., Beeler, N.M., Blanpied, M.L., 2000. On rate-state and Coulomb failure models. Journal of Geophysical Research 105, 7557–7871.

Gordon, R.B., 1967. Thermally activated processes in the Earth: creep and seismic attenuation. Geophysical Journal of the Royal Astronomical Society 14, 33–43.

Gu, J.C., Rice, J.R., Ruina, A.L., Tse, S.T., 1984. Slip motion and stability of a single degree of freedom elastic system with rate and state dependent friction. Journal of the Mechanics and Physics of Solids 32, 167–196. http://dx.doi.org/10.1016/0022-5096(84)90007-3.

Gutenberg, B., Richter, C.F., 1944. Frequency of earthquakes in California. Bulletin of the Seismological Society of America 34, 185–188.

Harris, R., 1998. Introduction to special section: stress triggers, stress shadows, and implications for seismic hazard. Journal of Geophysical Research 103, 24,347–24,358.

Heisenberg, W., 1927. Über den anschaulichen Inhalt der quantentheoretischen kinematik und mechanik. Zeitschrift für Physik 43 (3–4), 172–198.

Holm, R., 1946. Electric Contacts. H. Gebers Förlag, Stockholm . 398 pp.

Housner, G.W., Bergman, L.A., Caughey, T.K., Chassiakos, A.G., Claus, R.O., Masri, S.F., Skelton, R.E., Soong, T.T., Spencer, B.F., Yao, J.T.P., 1997. Structural control: past, present, and future. Journal of Engineering Mechanics (ASCE) 123 (9), 897–971. http://dx.doi.org/10.1061/(ASCE)0733-9399(1997)123:9(897).

Huang, J., Narkounskaia, G., Turcotte, D.L., 1992. A cellular-automata, slider-block model for earthquake II. Demonstration of self-organized criticality for a 2-D

system. Geophysical Journal International 111, 259–269. http://dx.doi.org/10.1111/j.1365-246X.1992.tb00575.x.
Hubbert, M.K., Rubey, W.W., 1959. Mechanics of fluid-filled porous solids and its application to overthrust faulting. Geological Society of America Bulletin 70, 115–166.
Hull, J., 1988. Thickness–displacement relationships for deformation zones. Journal of Structural Geology 10, 431–435. http://dx.doi.org/10.1016/0191-8141(88)90020-X.
Ida, Y., 1972. Cohesive force across the tip of a longitudinal−shear crack and Griffith's specific surface energy. Journal of Geophysical Research 77 (20), 3796–3805.
Ishibe, T., Shimazaki, K., 2012. Characteristic earthquake model and seismicity around late Quaternary active faults in Japan. Bulletin of the Seismological Society of America 102 (3), 1041–1058. http://dx.doi.org/10.1785/0120100250.
Jackson, D.D., Kagan, Y.Y., 2006. The 2004 Parkfield earthquake, the 1985 prediction, and characteristic earthquakes: lessons for the future. Bulletin of the Seismological Society of America 96 (4b), S397–S409.
Jeffreys, H., 1938. Aftershocks and periodicity in earthquakes. Gerlands Beitrage zur Geophysik 53, 111–139.
Jourde, H., Flodin, E.A., Aydin, A., Durlofsky, L.J., Wen, X.H., 2002. Computing permeability of fault zones in Eolian sandstone from outcrop measurements. AAPG Bulletin 86, 1187–1200.
Kagan, Y.Y., 1994. Observational evidence for earthquakes as a nonlinear dynamic process. Physica D 77 (1–3), 160–192.
Kagan, Y.Y., 1996. Comment on "The Gutenberg–Richter or characteristic earthquake distribution, which is it?" by S. G. Wesnousky. Bulletin of the Seismological Society of America 86, 274–285.
Kagan, Y.Y., Jackson, D.D., 1995. New seismic gap hypothesis: five years after. Journal of Geophysical Research 99, 3943–3959.
Kagan Y.Y., Jackson, D. D., Geller, R., in press. Characteristic earthquake model, 1884–2011, R. I. P. Seism. Res. Let., Opinion Letters.
Kanamori, H., 1981. The nature of seismicity patterns before large earthquakes. In: Simpson, D., Richards, P.G. (Eds.), Earthquake Prediction: An International Review. Maurice Ewing Set., 4. AGU, Washington, D.C., pp. 1–19.
Kanamori, H., 2003. Earthquake prediction: an overview. In: Lee, W.H.K., Kanamori, H., Jennings, P.C., Kisslinger, C. (Eds.), International Handbook of Earthquake & Engineering Seismology. Academic Press, San Diego, CA, pp. 1205–1216.
Kato, N., 2001. Effect of frictional heating on pre-seismic sliding: a numerical simulation using a rate-, state- and temperature-dependent friction law. Geophysical Journal International 147, 183–188.
Kawamura, H., Hatano, T., Kato, N., Biswas, S., Chakrabarti, B.K., 2012. Statistical physics of fracture, friction and earthquake. Reviews of Modern Physics 84 (2), 839–884. http://dx.doi.org/10.1103/RevModPhys.84.839.
Kelleher, J., Sykes, L.R., Oliver, J., 1973. Possible criteria for predicting earthquake locations and their application to major plate boundaries of the Pacific and the Caribbean. Journal of Geophysical Research 78, 2547–2585.
Klügel, J.-U., 2005. Problems in the application of the SSHAC probability method for assessing earthquake hazards at Swiss nuclear power plants. Engineering Geology 78, 285–307.
Klügel, J.-U., 2008. Seismic hazard analysis — Quo vadis? Earth-Science Reviews 88 (1–32).
Klügel, J.-U., 2011. Uncertainty analysis and expert judgement in seismic hazard analysis. Pure and Applied Geophysics 168.
Klügel, J.-U., Attinger, R., Rao, S., Vaidya, N., 2009. Adjusting the fragility method to the seismic hazard input. Part I: The intensity-based method. SMiRT, Espoo.
Kossobokov, V.G., Nekrasova, A.K., 2012. Global seismic hazard assessment program maps are erroneous. Seismic Instruments 48 (2), 162–170.
Kozeny, J., 1927. Uber kapillare leitung der wasser in boden. Sitzungsberichte der Akademie der Wissenschaften in Wien 136, 271e306 (in German).
Lachenbruch, A.H., 1980. Frictional heating, fluid pressure, and the resistance to fault motion. Journal of Geophysical Research 85, 6097–6122.
Langbein, J., Borcherdt, R., Dreger, D., 2005. Preliminary report on the 28 September 2004, M 6.0 Parkfield, California Earthquake. Seismological Research Letters 76, 10–26.
Lapusta, N., Barbot, S., 2012. Models of earthquakes and aseismic slip based on laboratory-derived rate and state friction laws. In: Bizzarri, A., Bhat, H.S. (Eds.), The Mechanics of Faulting: From Laboratory to Real Earthquakes: Ressign Post. ISBN: 978-81-308-0502-3.
Lapusta, N., Liu, Y., 2009. Three-dimensional boundary integral modeling of spontaneous earthquake sequences and aseismic slip. Journal of Geophysical Research 114, B09303. http://dx.doi.org/10.1029/2008JB005934.
Marone, C., Raleigh, B.B., Scholz, C.H., 1990. Frictional behavior and constitutive modeling of simulated gouge. Journal of Geophysical Research 95 (B5), 7007–7025. http://dx.doi.org/10.1029/095iB05p07007.
Marone, C., Vidale, J.E., Ellsworth, W., 1995. Fault healing inferred from time dependent variations in source properties of repeating earthquake. Geophysical Research Letters 22 (22), 3095–3098.
Marrett, R., Allmendinger, R.W., 1990. Kinematic analysis of fault-slip data. Journal of Structural Geology 12, 973–986. http://dx.doi.org/10.1016/0191-8141(90)90093-E.
Miller, S.A., Nur, A., Olgaard, D.L., 1996. Earthquakes as a coupled shear stress–high pore pressure dynamical system. Geophysical Research Letters 23, 197–200.
Mitsui, Y., Cocco, M., 2010. The role of porosity evolution and fluid flow in frictional instabilities: a parametric study using a spring–slider dynamic system. Geophysical Research Letters 37, L23305. http://dx.doi.org/10.1029/2010GL045672.
Mitsui, Y., Hirahara, K., 2009. Coseismic thermal pressurization can notably prolong earthquake recurrence intervals on weak rate and state friction faults: numerical experiments using different constitutive equations. Journal of Geophysical Research 114, B09304. http://dx.doi.org/10.1029/2008JB006220.
Mogi, K., 1985. Earthquake Prediction. Academic Press, London . 335 pp.
Molchan, G., Kronod, T., Panza, G.F., 1997. Multi-scale seismicity model for seismic risk. Bulletin of the Seismological Society of America 87 (5), 1220–1229.
Molnar, P., 1979. Earthquake recurrence intervals and plate tectonics. Bulletin of the Seismological Society of America 69 (1), 115–133.
Nadeau, R.M., Johnson, L.R., 1998. Seismological studies at Parkfield VI: moment release rates and estimates of source parameters for small repeating earthquake. Bulletin of the Seismological Society of America 88, 790–814.
Nakatani, M., 2001. Conceptual and physical clarification of rate and state friction: frictional sliding as a thermally activated rheology. Journal of Geophysical Research 106, 13,347–13,380. http://dx.doi.org/10.1029/2000JB900453.
Niemeijer, A., Marone, C., Ellsworth, D., 2010. Frictional strength and strain weakening in simulated fault gouge: competition between geometrical weakening and chemical strengthening. Journal of Geophysical Research 115, B10207. http://dx.doi.org/10.1029/2009JB000838.
Nishenko, S.P., 1989. Earthquakes, hazards and predictions. In: James, D.E. (Ed.), The Encyclopedia of Solid-Earth Geophysics. Van Nostrand Reinhold, New York, pp. 260–268.
Noda, H., Dunham, E.M., Rice, J.R., 2009. Earthquake ruptures with thermal weakening and the operation of major faults at low overall stress levels. Journal of Geophysical Research 114, B07302. http://dx.doi.org/10.1029/2008JB006143.
Norme tecniche di costruzione, 2008. D.M. 14/01/08, Gazzetta Ufficiale No. 29, 04/02/08 (http://www.gazzettaufficiale.it/).
Okada, T., Matsuzawa, T., Hasegawa, A., 2003. Comparison of source areas of M4.8 +/− 0.1 repeating earthquakes off Kamaishi, NE Japan: are asperities persistent features? Earth and Planetary Science Letters 213 (3–4), 361–374. http://dx.doi.org/10.1016/S0012-821X(03000299-1.
Panza, G.F., Romanelli, F., Vaccari, F., 2001. Seismic wave propagation in laterally heterogeneous anelastic media: theory and applications to seismic zonation. Advances in Geophysics 43, 1–95.
Panza, G.F., Irikura, K., Kouteva, M., Peresan, A., Wang, Z., Paragoni, R., 2011. Advanced seismic hazard assessment. Pure and Applied Geophysics 169, 1–9. http://dx.doi.org/10.1007/s00024-010-0179-9.
Panza, G.F., La Mura, C., Peresan, A., Romanelli, F., Vaccai, F., 2012. Seismic hazard scenarios as preventive tools for a disaster resilient society. Advances in Geophysics 53, 93–165.
Paterson, M.S., Wong, T.-F., 2005. Experimental rock deformation. Springer, The Netherlands. 347 pp.
Power, W.L., Tullis, T.E., Weeks, D.J., 1988. Roughness and wear during brittle faulting. Journal of Geophysical Research 93 (B12), 15,268–15,278. http://dx.doi.org/10.1029/JB093iB12p15268.
Press, W.H., Teukolsky, B.P., Vetterling, W.T., 1992. Numerical Recipes, 2nd ed. Cambridge University Press, New York.
Rathbun, A.P., Marone, C., 2010. Effect of strain localization on frictional behavior of sheared granular materials. Journal of Geophysical Research 115, B01204. http://dx.doi.org/10.1029/2009JB006466.
Reid, H.F., 1910. The California earthquake of April 18, 1906. Report of the State Investigation Commission. The Mechanics of the Earthquake, vol. 2. Carnegie Inst., Washington, D. C.
Rice, J.R., 1992. Fault stress states, pore pressure distributions, and the weakness of the San Andreas Fault. In: Evans, B., Wong, T.-F. (Eds.), Fault Mechanics and Transport Properties in Rocks. Academic, San Diego, CA, USA, pp. 475–503.
Rice, J.R., Gu, J., 1983. Earthquake after effects and triggered seismicity phenomena. Pure and Applied Geophysics 121, 187–219.
Robertson, E.C., 1983. Relationship of fault displacement to gouge and breccia thickness. Mining Engineering 35, 1426–1432.
Roy, M., Marone, C., 1996. Earthquake nucleation on model faults with rate and state-dependent friction: effects of inertia. Journal of Geophysical Research 101, 13,919–13,932.
Rubin, A.M., Ampuero, J.-P., 2005. Earthquake nucleation on (aging) rate and state faults. Journal of Geophysical Research 110, B11312. http://dx.doi.org/10.1029/2005JB003686.
Ruina, A.L., 1983. Slip instability and state variable friction laws. Journal of Geophysical Research 88, 10359–10370.
Rundle, J.B., Turcotte, D.L., Shcherbakov, R., Klein, W., Sammis, C., 2003. Statistical physics approach to understanding the multiscale dynamics of earthquake fault systems. Reviews of Geophysics 41 (4), 1019. http://dx.doi.org/10.1029/2003RG000135.
Rybicki, K., Sato, T., Kasahara, K., 1985. Mechanical interaction between neighboring active faults: static and dynamic stress field induced by faulting. Bulletin of the Earthquake Research Institute, University of Tokyo 60, 1–21.
Saito, T., Matsukawa, H., 2007. Size dependence of the Burridge–Knopoff model. Journal of Physics Conference Series 89, 012016. http://dx.doi.org/10.1088/1742-6596/89/1/012016.
Samuelson, J., Ellsworth, D., Marone, C., 2009. Shear-induced dilatancy of fluid saturated faults: experiment and theory. Journal of Geophysical Research 114, B12404. http://dx.doi.org/10.1029/2008JB006273.
Scholz, C.H., 2002. The Mechanics of Earthquakes and Faulting, 2nd ed. Cambridge Univ. Press, Cambridge. U. K. 473 pp.
Schwartz, D.P., Coppersmith, K.S., 1984. Fault behavior and characteristic earthquakes: examples from the Wasatch and San Andreas fault zones. Journal of Geophysical Research 89, 5681–5698.
Seeton, C.J., 2006. Viscosity–temperature correlation for liquids. Tribology Letters 22 (1). http://dx.doi.org/10.1007/s11249-006-9071-2.
Segall, P., Rice, J.R., 1995. Dilatancy, compaction, and slip instability of a fluid-infiltrated fault. Journal of Geophysical Research 100, 22,155–22,171.

Shapiro, S.A., Patzig, R., Rothert, E., Rindshwentner, J., 2003. Triggering of seismicity by pore-pressure perturbations: permeability-related signature of the phenomenon. Pure and Applied Geophysics 160, 1051–1066.

Shearer, R., 1985. Minutes of the National Earthquake Prediction Evaluation Council (NEPEC). Open-File Rep. U.S. Geol. Surv. pp. 85–507.

Shimazaki, K., Nakata, T., 1980. Time-predictable model for large earthquakes. Geophysical Research Letters 7, 279–282. http://dx.doi.org/10.1029/GL007i004p00279.

Sleep, N.H., 1995. Ductile creep, compaction, and rate and state dependent friction within major fault zones. Journal of Geophysical Research 100 (B7), 13,065–13,080.

Sleep, N.H., 1997. Application of a unified rate and state friction theory to the mechanics of fault zones with strain localization. Journal of Geophysical Research 102, 2875–2895.

Sone, H., Shimamoto, T., 2009. Frictional resistance of faults during accelerating and decelerating earthquake slip. Nature Geoscience. http://dx.doi.org/10.1038/NGEO637.

Stein, R.S., 1999. The role of stress transfer in earthquake occurrence. Nature 402, 605–609.

Sykes, L.R., Menke, W., 2006. Repeat times of large earthquakes: implications for earthquake mechanics and long-term prediction. Bulletin of the Seismological Society of America 96 (5), 1569–1596. http://dx.doi.org/10.1785/0120050083.

Tse, S.T., Rice, J.R., 1986. Crustal earthquake instability in relation to the depth variation of frictional slip properties. Journal of Geophysical Research 91, 9452–9472. http://dx.doi.org/10.1029/JB091iB09p09452.

Turcotte, D.L., 1997. Fractals and Chaos in Geology and Geophysics, 2nd edition. Cambridge Univ. Press, N.Y.

Turcotte, D.L., Shcherbakov, R., Rundle, J.B., 2009. In: Kanamori, H. (Ed.), Treatise on Geophysics, 4. Elsevier, Amsterdam, pp. 675–700.

Vere-Jones, D., 2010. Foundations of statistical seismology. Pure and Applied Geophysics 167, 645–653. http://dx.doi.org/10.1007/s00024-010-0079-z.

Walsh, J.B., 1971. Stiffness in faulting and in friction experiments. Journal of Geophysical Research 76 (35), 8597–8598.

Wang, Z., 2008. Understanding seismic hazard and risk: a gap between engineers and seismologists. The 14th world conference on earthquake engineering. October 12–17. 2008. Beijing, China (Paper No. S27-001).

Weeks, J.D., 1993. Constitutive laws for high-velocity frictional sliding and their influence on stress drop during unstable slip. Journal of Geophysical Research 98, 17,637–17,648.

Wibberley, C.A.J., Shimamoto, T., 2003. Internal structure and permeability of major strike-slip fault zones: the Median Tectonic Line in Mie Prefecture, Southwest Japan. Journal of Structural Geology 25, 59–78.

Wyss, M., Nekrasova, A., Kossobokov, V., 2012. Errors in expected human losses due to incorrect seismic hazard estimates. Natural Hazards. http://dx.doi.org/10.1007/s11069-012-0125-5.

Yamashita, T., 1998. Simulation of seismicity due to fluid migration in a fault zone. Geophysical Journal International 132, 661–675.

Zechar, J.D., Nadeau, R.M., 2012. Predictability of repeating earthquakes near Parkfield, California. Geophysical Journal International 190, 457–461. http://dx.doi.org/10.1111/j.1365-246X.2012.05481.x.

Zhang, S., Tullis, T.E., Scruggs, V.J., 1999. Permeability anisotropy and pressure dependency of permeability in experimentally sheared gouge materials. Journal of Structural Geology 21, 795–806.

Zuccolo, E., Vacari, F., Peresan, A., Panza, G.F., 2011. Neo-deterministic and probabilistic hazard assessements: a comparison over the Italian territory. Pure and Applied Geophysics 168, 69–83. http://dx.doi.org/10.1007/s.00024-010-0151-8.